Physics and Chemistry of the Earth 136 (2024) 103783

Contents lists available at ScienceDirect

Physics and Chemistry of the Earth

journal homepage: www.elsevier.com/locate/pce

Characterization of water-soluble inorganic ions and carbonaceous aerosols in the urban atmosphere in Amman, Jordan

Afnan Al-Hunaiti [a,b], Zaid Bakri [c], Xinyang Li [d], Lian Duan [d,e], Asal Al-Abdallat [f], Andres Alastuey [g], Mar Viana [g], Sharif Arar [a], Tuukka Petäjä [d], Tareq Hussein [d,f,*]

[a] Department of Chemistry, School of Science, University of Jordan, 11942, Amman, Jordan
[b] Department of Chemistry and Materials Science, School of Chemical Engineering, Nanochemistry and Nanoengineering, Aalto University, Aalto, 00076, Finland
[c] Department of Physics and Atmospheric Sciences Program, Michigan Technological University, Houghton, MI, 49931, USA
[d] University of Helsinki, Institute for Atmospheric and Earth System Research (INAR/Physics), UHEL, FI-00014, Helsinki, Finland
[e] Shanghai Key Laboratory of Atmospheric Particle Pollution and Prevention, Department of Environmental Science & Engineering, Fudan University, Shanghai, 200438, China
[f] Environmental and Atmospheric Research Laboratory (EARL), Department of Physics, School of Science, University of Jordan, Amman, 11942, Jordan
[g] Institute of Environmental Assessment and Water Research (IDAEA-CSIC), 08034, Barcelona, Spain

ARTICLE INFO

Keywords:
Urban air quality
Particulate matter
Inorganic
Ions
Carbonaceous aerosols
SDS

ABSTRACT

The urban particulate matter (PM) carbonaceous and water-soluble ions were investigated in Amman, Jordan during May 2018–March 2019. The $PM_{2.5}$ total carbon (TC) annual mean was 7.6 ± 3.6 μg/m^3 (organic carbon (OC) 5.9 ± 2.8 μg/m^3 and elemental carbon (EC) 1.7 ± 1.1 μg/m^3), which was about 16.3% of the $PM_{2.5}$. The PM_{10} TC annual mean was 8.4 ± 3.9 μg/m^3 (OC 6.5 ± 3.1 μg/m^3 and elemental carbon (EC) 1.9 ± 1.1 μg/m^3), about 13.3% of the PM_{10}. The $PM_{2.5}$ total water-soluble ions annual mean was 7.9 ± 1.9 μg/m^3 (about 16.9%), and that of the PM_{10} was 10.1 ± 2.8 μg/m^3 (about 16.0%). The minor ions (F^-, NO_2^-, Br^-, and PO_4^{3-}) constituted less than 1% in the PM fractions. The significant fraction was for SO_4^{2-} ($PM_{2.5}$ 4.7 ± 1.6 μg/m^3 (10.0%) and PM_{10} 5.3 ± 1.9 μg/m^3 (8.3%)). The NH_4^+ had higher amounts of $PM_{2.5}$ (1.3 ± 0.6 μg/m3; 2.7%) than that PM_{10} (0.9 ± 0.4 μg/m^3; 1.4%). During sand and dust storm (SDS) events, TC, Cl^-, and NO_3^- were doubled in PM, SO_4^{2-} did not increase significantly, and NH_4^+ slightly decreased. Regression analysis revealed: (1) carbonaceous aerosols come equally from primary and secondary sources, (2) about 50% of the OC came from non-combustion sources, (3) traffic emissions dominate the PM, (4) agricultural sources have a negligible effect, (5) SO_4^{2-} is completely neutralized by NH_4^+ in the $PM_{2.5}$ but there could be additional reactions involved in the PM_{10}, and (6) $(NH_4)_2SO_4$, was the major species formed by $SO_4^{2-}$and NH_4^+ instead of NH_4HSO_4. It is recommended to perform long-term sampling and chemical speciation for the urban atmosphere in Jordan.

1. Introduction

Long periods of drought could also increase air pollutants and that was indicated in lower organic matter content within pollen traps in the year 2010–2011 compared to 2009–2010 by 9.9% (Al-Dousari et al., 2018). The long drought periods, water scarcity, and the huge precipitation variations are enhancing aeolian activities as part of pollutants on the regional scale (Doronzo et al., 2016).

Salts (such as SO_4^{2-}, NO_3^-, Cl^-, and NH_4^+) are observed to constitute the majority of the inorganic ions in fine particulate matter ($PM_{2.5}$), accounting for more than 80% of all water-soluble inorganic ions (WSIIs) (Tsai et al., 2021). WSIIs impact air quality, visibility, health, and climate (Delfino et al., 2005; Goudarzi et al., 2019; Hong et al., 2022; Khan et al., 2010; Komaba and Fukagawa, 2016; Naimabadi et al., 2016; Organización Mundial de la Salud, 2021; Pui et al., 2014; Zhang et al., 2011). For example, some WSIIs are known for causing smog when relative humidity exceeds 60%. Furthermore, their light extinction coefficient is relatively high, and plays a major role in reducing visibility in many cities (Hong et al., 2022). SO_4^{2-} contributes to the effect of acid rain, while phosphate (PO_4^{3-}) can harm the cardiovascular system in

* Corresponding author. University of Helsinki, Institute for Atmospheric and Earth System Research (INAR/Physics), UHEL, FI-00014, Helsinki, Finland.
E-mail addresses: a.alhunaiti@ju.edu.jo (A. Al-Hunaiti), zbakri@mtu.edu (Z. Bakri), xinyang.li@helsinki.fi (X. Li), lian.duan@helsinki.fi, lduan20@fudan.edu.cn (L. Duan), asl9170208@ju.edu.jo (A. Al-Abdallat), andres.alastuey@idaea.csic.es (A. Alastuey), mar.viana@idaea.csic.es (M. Viana), s.arar@ju.edu.jo (S. Arar), tuukka.petaja@helsinki.fi (T. Petäjä), tareq.hussein@helsinki.fi, t.hussein@ju.edu.jo (T. Hussein).

https://doi.org/10.1016/j.pce.2024.103783
Received 3 June 2024; Received in revised form 10 October 2024; Accepted 18 October 2024
Available online 20 October 2024

humans and animals as well (Komaba and Fukagawa, 2016). Excessive emissions of some ions (e.g. NO_2^-) potentially alter the ozone cycle in addition to its contribution to the absorption of visible solar radiation, which has two consequences: (1) impaired atmospheric visibility, and (2) contribution to global warming (Organización Mundial de la Salud (OMS), 2021).

Contrary to carbonaceous aerosols, sources of atmospheric WSIIs are relatively easier to identify. The common sources of WSIIs in the atmosphere are either natural sources (e.g., photochemical reactions, the NO_x cycle in the atmosphere, and certain microbiological activities) or anthropogenic sources and processes. (Freyer et al., 1993; Gupta et al., 2023; Lestari et al., 2024; Pui et al., 2014; Tran et al., 2024; Williams et al., 2021; YAHAYA et al., 2023). For example, PO_4^{3-} is commonly emitted during fertilizer production (YAHAYA et al., 2023). NO_2^-, NO_3^-, and NH_4^+ are agents in the primary chemical reactions and cycles in the atmosphere and the production of other nutrients such as N_2. SO_4^{2-}, NO_3^-, and NH_4^+ are significant precursors for secondary inorganic aerosol (SIA) formation. Elevated concentrations of NO_3^- and SO_4^{2-} are influenced by meteorological factors that enhance oxidation rates of NO_2 and SO_2. NH_4^+ is formed through the conversion of NH_3, mainly contributed by agriculture and vehicle exhaust (Rattanapotanan et al., 2023).

The Mediterranean basin, where the northern Sahara of the African continent meets the southern coastal lands of southern Europe and the Levantine coast (i.e., the eastern Mediterranean), is considered a typical example of the long-range transport of many species of air pollutants carried by dust particles during sand and dust storm (SDS) episodes (Bozkurt, 2018; Cheng et al., 2022; Galindo et al., 2020; F.F. Ghasemi et al., 2023a,b; Goudarzi et al., 2019; Hussein et al., 2022; Naimabadi et al., 2016). These events have a substantial impact on the concentrations of the carbonaceous and non-carbonaceous aerosol species (Behrooz et al., 2017; Bozkurt, 2018; Cheng et al., 2022; F.F. Ghasemi et al., 2023a,b; Remoundaki et al., 2013; Saraga et al., 2017; Shahsavani et al., 2012; Tepe and Doğan, 2021). However, these previous studies reporting the chemical characterization focusing on WSIIs did not include urban areas within the Levant. It was only recently when we previously considered an urban area in Jordan affected by SDS episodes originating from different major sources of dust and classified into three main categories: S (Sahara), SL (Saharan and Levant), SA (Sahara and Arabia), and SLA (Sahara, Levant, and Arabia) (Hussein et al., 2020, 2022). In these previous two studies, we presented the PM2.5 and PM10 concentrations during these SDS events with chemical characterization of carbonaceous aerosols. There is a clear gap in scientific knowledge about the WSIIs in the Levant.

In this study, we present, for the first time the concentrations of OCEC and WSIIs as observed in PM2.5 and PM10 collected at an urban site in Amman, Jordan. The characterization of WSIIs was investigated with respect to previously classified SDS episodes. We explore the sources of aerosol particles based on their chemical composition and provide an assessment of aerosol sources in the region.

2. Materials and methods

2.1. Aerosol measurement

The aerosol measurement campaign was conducted from May 2018–March 2019 on the rooftop of the Department of Physics at the University of Jordan [32.0129 N°, 35.8738 E°]. The measurements were conducted approximately 20 m above the ground. The site was categorized as having an urban background location in the northern region of Amman, Jordan. The surrounding area consisted of a blend of residential areas and a network of roads.

The aerosol measurement instrumentation included two high-volume samplers (model CAV-A/mb, MCV, S.A., Spain) and a cascade head (model PM1025-CAV, MCV, S.A.) to collect filter samples for PM_{10} and $PM_{2.5}$. The filter media used in these samplers was quartz (Pallflex, PALLXQ250ETDS0150, TISSUQUARTZ 2500 QAT-UP) with a diameter of 15 cm. The sampling flow rate was set to 30 m3 h–1, and the sampler automatically recorded the overall mean ambient temperature and atmospheric pressure during the sampling sessions.

Each sample was collected over 24 h every 6 days. Accordingly, we acquired 51 and 48 valid samples of PM_{10} and $PM_{2.5}$, respectively. Additionally, we collected six blank samples.

2.2. Gravimetric and PM chemical composition analysis

Before the chemical composition analysis of the PM samples, gravimetric analysis was performed to determine the PM_{10} and $PM_{2.5}$ mass concentrations according to the European directive EN1234-1. Accordingly, the particulate matter concentration can be calculated from the filter weights (difference between post-sampling (weight m_{post}) and pre-sampling (weight m_{pre})) divided by the sampling flow rate (Q [30 m^3 h^{-1}]) and sampling period (Δt [24 h]).

After the determination of the air sample mass, a 1/4 fraction of each filter was bulk acid digested and leached to extract WSIIs (F^-, Cl^-, NO_2^-, Br^-, NO_3^-, PO_4^{3-}, SO_4^{2-} and NH_4^+) and subsequent analysis by ion chromatography (IC) and flow injection analysis (FIA). Another 1/4 of the sampled filter was taken to the OC and EC analysis according to the EUSAAR2 protocol employing a Sunset Laboratory Dual-Optical Carbonaceous Analyzer (Birch and Cary, 1996; Cavalli et al., 2010; Viana et al., 2007a).

The results of ion concentrations from IC were expressed in ppm, and the ppm-μg/m^3 conversion was processed using the blank sample concentration (C_{blk}), leachate volume ($V_l = 30$ m^3), sample filter portion (p = 4, ¼ filters per analysis) and total sampled air volume ($V_{air} = Q^*\Delta t$ = 720 m^3). The equation for the ion concentration calculation is shown as follows:

$$C_{ion}\left[\frac{\mu g}{m^3}\right] = \frac{C_{ion}[ppm] - C_{blk}[ppm]}{V_{air}} \times V_l \times p \tag{1}$$

2.3. Weather conditions

In addition to the aerosol measurement, the ambient meteorology conditions (Temperature, Pressure, Relative Humidity, Wind Speed and Wind Direction, and precipitation) were monitored with a 5-min resolution by using a weather station (WH-1080, Clas Ohlson: Art. no. 36–3242).

The monthly mean ambient temperature (T) was around 24 °C during the summer and around 9 °C in winter. Throughout the campaign (May 2018–March 2019), the daily mean T was in the range of 3–30 °C (overall mean 17 ± 7 °C). The monthly mean relative humidity (RH) was about 55% and 82% during the summer and the winter; respectively. The daily mean RH was in the range 20–100% (overall mean 68 ± 21%). The absolute pressure (P) was about 896 hPa and 901 hPa during the summer and the winter; respectively. The daily mean P was in the range 890–908 hPa (overall mean 899 ± 4 hPa). The monthly mean wind speed (WS) during the autumn (September–November) was lower than in the summer. The maximum monthly WS was reported 2.1 m/s in August, and the minimum was 0.8 m/s in November.

By the end of the measurement campaign, the cumulative precipitation was about 470 mm. The rainy season started in October 2018 with a small amount (cumulative ~13 mm). During December 2018, the cumulative precipitation was about 180 mm. During January–February 2019, the cumulative precipitation was about 120 mm.

3. Results

3.1. An overview of the PM concentrations

Our results show that the particulate matter (PM_{10} and $PM_{2.5}$) concentrations were below 200 μg/m^3 during the measurement period (Fig. 1). On average, the $PM_{2.5}$ concentration was 47 ± 32 μg/m^3 and

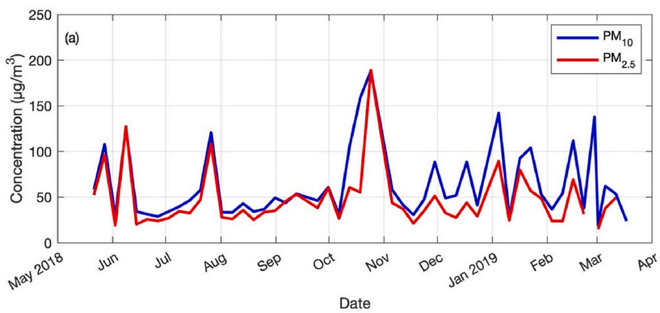

Fig. 1. Concentrations of 24-h average PM_{10} and $PM_{2.5}$ during the measurement period. The Sand and Dust Storm (SDS) events were chosen when $PM_{10} >$ 70 µg/m^3. During the sampling period, ten SDS were observed.

the PM_{10} was about 63 ± 39 µg/m^3 with an overall ratio $PM_{2.5}/PM_{10}$ about 0.74 (Table 1) indicating the dominance of fine particulate matter (PM2.5). The minimum concentration was 19 µg/m^3 and 15 µg/m^3, respectively, for PM_{10} and $PM_{2.5}$.

The aerosol mass concentrations in the region were influenced by frequent Sand and Dust Storms (SDS); in total ten SDS were observed. Here, SDS events were identified when PM_{10} exceeded 70 µg/m^3 based-on visual observation during the sampling. For example, on October 23, 2018, a severe SDS was observed with a concentration of around 189 µg/m^3 for both PM_{10} and $PM_{2.5}$. In general, the PM_{10} and $PM_{2.5}$ concentrations were increased during SDS events and the ratio $PM_{10}/PM_{2.5}$ was generally larger indicating a larger relative contribution of larger dust particles than one except for that severe event on October 23rd.

The carbonaceous and water-soluble conistituients will be presented and discussed in detail in the following subsections. The remaining contents, mainly mineral-related elements and trace metals, indicated by "others," were not identified according to our analytical procedure. On average, this remaining fraction accounts for about 67% and 70% of the $PM_{2.5}$ and PM_{10}, respectively.

3.2. Chemical characterization

3.2.1. Elemental and organic carbon

Since the SDS event on October 23 was a severe event, it was excluded from further analysis. Accordingly, the total carbon (TC) concentration in the fine fraction ($PM_{2.5}$) was in the range 1.7–13.6 µg/m^3. The overall average TC was 7.6 ± 3.6 µg/m^3, accounting for 16.3% of the $PM_{2.5}$ content (Fig. 2b and Table 1). The elemental carbon (EC) constitutes about 1.7 ± 1.1 µg/m^3 (3.5% of $PM_{2.5}$) whereas the organic carbon (OC) was 5.9 ± 2.8 µg/m^3 (12.7% of $PM_{2.5}$); see Fig. 3.

Similarly, PM_{10} TC content ranged from 2.7 to 20.0 µg/m^3. The overall average TC was 8.4 ± 3.9 µg/m^3, accounting for 13.3% of PM_{10}

Table 1
Overall particulate matter (PM_{10} and $PM_{2.5}$) concentrations (µg/m^3) and their carbon and water-soluble ions contents with the corresponding percentage.

	$PM_{2.5}$			PM_{10}			$\frac{PM_{2.5}}{PM_{10}}$
	Mean	Std	%	Mean	Std	%	
PM_x	46.75	31.96		62.97	39.40		0.74
EC [a]	1.65	1.08	3.54	1.90	1.08	3.01	0.87
OC [b]	5.94	2.79	12.71	6.48	3.08	10.29	0.92
Cl^-	0.23	0.16	0.49	0.60	0.50	0.96	0.38
NO_3^-	1.64	0.92	3.50	3.29	1.96	5.23	0.50
SO_4^{2-}	4.68	1.59	10.02	5.25	1.86	8.34	0.89
NH_4^+	1.27	0.60	2.71	0.88	0.44	1.40	1.44
Other Ions [c]	0.06	0.02	0.13	0.06	0.03	0.10	1.01
Others	31.30	28.84	66.91	44.52	35.32	70.70	0.70

[a] EC: elemental carbon.
[b] OC: elemental carbon.
[c] Other ions include F^-, NO_2^-, Br^-, and PO_4^{3-}.

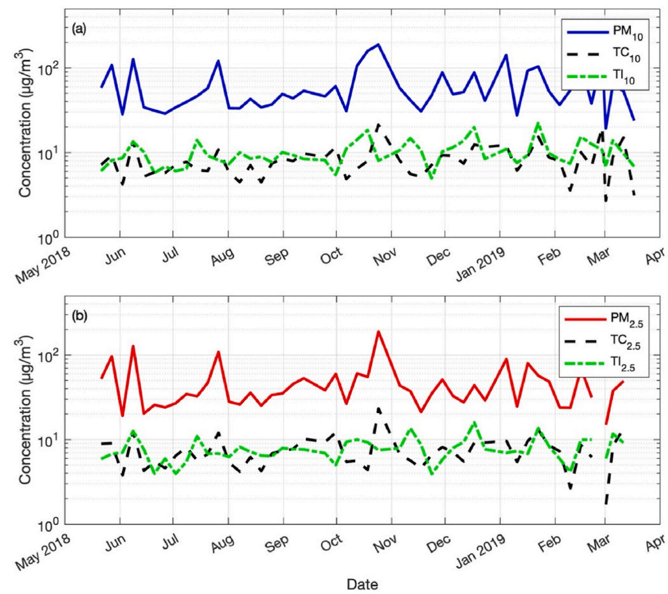

Fig. 2. Concentrations of total carbon (TC) and total ions (TI) with corresponding (a) PM_{10} and (b) $PM_{2.5}$ during the measurement period.

(Fig. 2a and Table 1). The PM_{10} EC constitutes about 1.9 ± 1.1 µg/m^3 (3.0%), whereas the OC was 6.5 ± 3.1 µg/m^3 (10.3%); see also Fig. 3.

In both the PM_{10} and $PM_{2.5}$ the EC fraction was less than the OC fraction (Fig. 4). The TC, EC, and OC concentrations were also higher in the PM_{10} than in the $PM_{2.5}$; ratios respectively were 0.91, 0.87, and 0.92 (Table 1). However, the TC, EC, and OC percentage was slightly lower in the PM_{10} than in the $PM_{2.5}$. This is expected because the coarse fraction is expected to include more fractions of other components than the carbonaceous contents.

3.2.2. Water-soluble ions

Excluding the severe SDS event on October 23, 2018, the total water-soluble ions (TI) was about 7.9 ± 1.9 µg/m^3 (about 16.9%) and 10.1 ± 2.8 µg/m^3 (about 16.0%); respectively in the $PM_{2.5}$ and PM_{10} (Table 1, Fig. 3). The TI amount was relatively similar to those for the TC within the $PM_{2.5}$ but they were less within the PM_{10}. The minor ions (F^-, NO_2^-, Br^-, and PO_4^{3-}) constituted less than 1% in the PM fractions. The significant fraction among all ions was found for SO_4^{2-} with an overall average 4.7 ± 1.6 µg/m^3 (10.0%) in $PM_{2.5}$ and 5.3 ± 1.9 µg/m^3 (8.3%) in PM_{10} (Table 1).

The ions Cl^-, NO_3^- and SO_4^{2-} amounts within the $PM_{2.5}$ (0.2 ± 0.2, 1.6 ± 0.9, and 4.7 ± 1.6; respectively) were less than those within the PM_{10} (0.6 ± 0.5, 3.3 ± 2.0, and 5.3 ± 1.9; respectively) (Table 1). Interestingly, the SO_4^{2-} percentage fraction within the $PM_{2.5}$ (about 10%) was more significant than that within the PM_{10} (about 8%), indicating that this water-soluble ion is mainly concentrated within the fine fraction. An interesting thing was found for NH_4^+, which had a higher mass concentration within the $PM_{2.5}$ (average 1.3 ± 0.6 µg/m^3; about 2.7%) than that within the PM_{10} (average 0.9 ± 0.4 µg/m^3; about 1.4%) indicating that this water-soluble ion is reactive with other components in the coarse fraction.

3.3. Warm versus cold conditions

Taking into consideration the conditions with temperature T > 15 °C (warm) versus temperature T < 9 °C (cold) revealed that the PM (both $PM_{2.5}$ and PM_{10}) concentrations were relatively higher during warm conditions. However, the chemical characteristics changed significantly with respect to EC and some major water-soluble ions (including Cl^-, NO_3^-, and NH_4^+).

The concentrations of EC and some water-soluble ions (Cl^-, NO_3^-,

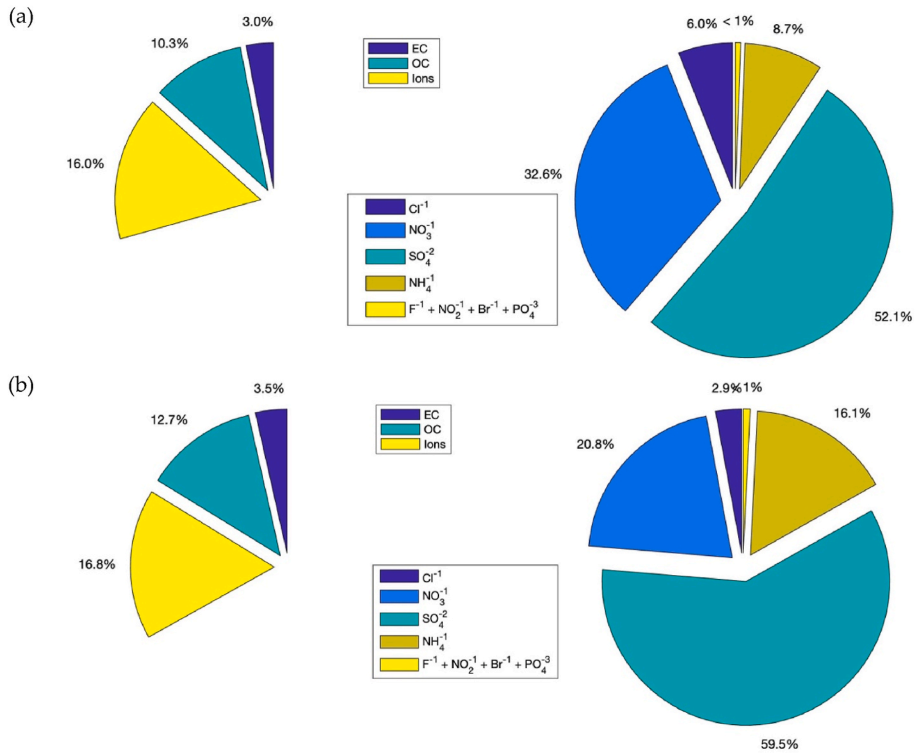

Fig. 3. Chemical speciation for (**a**) PM_{10} and (**b**) $PM_{2.5}$.

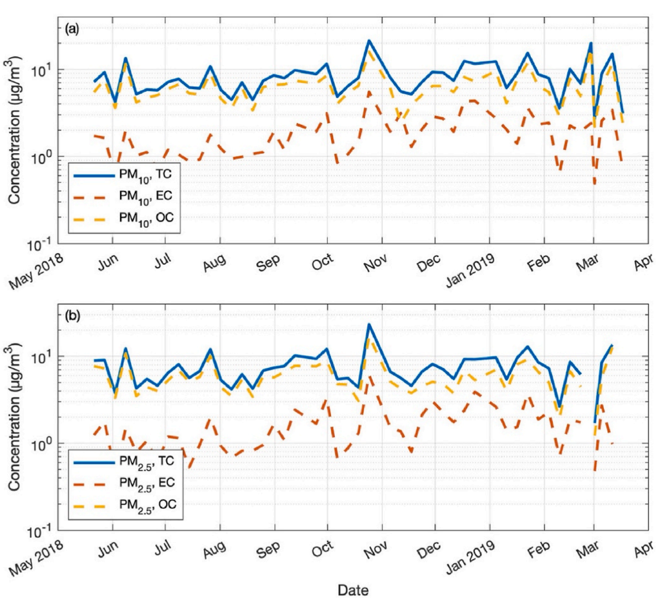

Fig. 4. Carbonaceous concentrations as total carbon (TC), elemental carbon (EC), and organic carbon (OC) in the (a) PM_{10} and (b) $PM_{2.5}$ during the measurement period.

and NH_4^+) were higher during cold conditions than during warm conditions (Tables 2 and 3, Fig. S1). The OC and other water-soluble ions (SO_4^{2-} and other ions including F^-, NO_2^-, Br^-, and PO_4^{3-}) did not significantly change between warm and cold conditions.

3.4. The influence of sand and dust storm (SDS) events

An interesting part of the analysis is to consider comparing the conditions with SDS events against clean air conditions. The picture is clear regarding the PM concentrations, which almost tripled (Tables 4 and 5, Fig. S2). The concentrations of the unknown components (indicated as "others") were quadrupled.

With respect to the PM_{10} contents of PM components analyzed (Table 4), the EC, OC, Cl^-, and NO_3^- almost doubled concentrations during SDS events. Whereas the concentrations of SO_4^{2-} did not increase significantly during SDS events compared to conditions without SDS events. The concentrations of NH_4^+ slightly decreased during SDS events.

As for the $PM_{2.5}$ contents (Table 5), the EC, OC, Cl^-, and NO_3^- almost doubled concentrations during SDS events, which is similar to that of PM_{10}. Meanwhile, the concentrations of SO_4^{2-} did not increase significantly, and that of NH_4^+ slightly decreased during SDS events when compared to conditions without SDS events. The other minor water-soluble ions (F^-, NO_2^-, Br^-, and PO_4^{3-}) increased by a factor of 1.6 during SDS events for $PM_{2.5}$ and PM_{10}.

Table 2
PM_{10} concentrations (μg/m^3) and their chemical contents and corresponding percentage during warm and cold conditions.

	Cold [a]			Warm [b]			cold/warm
	Mean	Std	%	Mean	Std	%	
PM_{10}	60.04	34.75		62.79	43.64		0.96
EC [c]	2.22	1.07	3.70	1.52	0.99	2.41	1.47
OC [d]	6.39	2.89	10.64	6.37	2.67	10.15	1.00
Cl^-	1.03	0.50	1.72	0.33	0.26	0.52	3.16
NO_3^-	3.69	2.66	6.14	2.82	1.19	4.49	1.31
SO_4^{2-}	5.18	1.63	8.63	5.17	1.89	8.24	1.00
NH_4^+	0.95	0.45	1.58	0.77	0.35	1.23	1.22
Other Ions [e]	0.06	0.02	0.10	0.06	0.03	0.10	0.90
Others	40.54	30.62	67.52	45.76	39.67	72.88	0.89

[a] Cold was taken with daily mean temperature T < 9 °C.
[b] Warm was taken with daily mean temperature T > 15 °C.
[c] EC: elemental carbon.
[d] OC: elemental carbon.
[e] Other ions include F^-, NO_2^-, Br^-, and PO_4^{3-}.

Table 3
$PM_{2.5}$ concentrations (μg/m^3) and their chemical contents and corresponding percentage during warm and cold conditions.

	Cold [a]			Warm [b]			cold/warm
	Mean	Std	%	Mean	Std	%	
$PM_{2.5}$	42.58	22.37		51.01	39.15		0.83
EC [c]	1.99	0.98	4.68	1.41	1.15	2.76	1.42
OC [d]	5.77	2.84	13.56	6.27	3.03	12.29	0.92
Cl^-	0.37	0.16	0.86	0.14	0.09	0.27	2.61
NO_3^-	2.05	0.98	4.82	1.26	0.64	2.47	1.63
SO_4^{2-}	4.48	1.36	10.52	4.75	1.54	9.32	0.94
NH_4^+	1.36	0.53	3.20	1.08	0.40	2.12	1.26
Other Ions [e]	0.06	0.01	0.13	0.07	0.03	0.13	0.87
Others	26.52	20.22	62.27	36.06	35.01	70.69	0.74

[a] Cold was taken with daily mean temperature T < 9 °C.
[b] Warm was taken with daily mean temperature T > 15 °C.
[c] EC: elemental carbon.
[d] OC: elemental carbon.
[e] Other ions include F^-, NO_2^-, Br^-, and PO_4^{3-}.

Table 4
PM_{10} concentrations (μg/m^3) and their chemical contents and corresponding percentage during conditions with SDS events and days without SDS events.

	Without SDS [a]			SDS [b]			SDS/nonSDS
	Mean	Std	%	Mean	Std	%	
PM_{10}	36.51	7.94		120.98	29.46		3.31
EC [c]	1.50	0.89	4.11	2.54	1.28	2.10	1.70
OC [d]	4.91	1.48	13.45	9.59	3.67	7.92	1.95
Cl^-	0.48	0.43	1.33	0.77	0.53	0.64	1.59
NO_3^-	2.52	0.92	6.91	4.89	2.76	4.05	1.94
SO_4^{2-}	4.90	1.60	13.42	6.43	2.31	5.32	1.31
NH_4^+	0.93	0.43	2.56	0.81	0.54	0.67	0.87
Other Ions [e]	0.05	0.01	0.13	0.08	0.03	0.06	1.62
Others	21.22	6.04	58.14	95.87	28.70	79.24	4.52

[a] Conditions without Sand and Dust Storm (SDS) events were taken with respect to $PM_{10} < 50$ μg/m^3.
[b] Conditions with SDS events were taken with respect to $PM_{10} > 70$ μg/m^3.
[c] EC: elemental carbon.
[d] OC: elemental carbon.
[e] Other ions include F^-, NO_2^-, Br^-, and PO_4^{3-}.

Table 5
$PM_{2.5}$ concentrations (μg/m^3) and their chemical contents and corresponding percentage during conditions with SDS events and days without SDS events.

	Without SDS [a]			SDS [b]			SDS/nonSDS
	Mean	Std	%	Mean	Std	%	
$PM_{2.5}$	29.08	7.00		85.58	41.19		2.94
EC [c]	1.26	0.77	4.33	2.39	1.41	2.80	1.90
OC [d]	4.69	1.32	16.13	8.00	3.63	9.35	1.71
Cl^-	0.17	0.14	0.60	0.30	0.17	0.36	1.74
NO_3^-	1.19	0.67	4.08	2.39	0.87	2.79	2.01
SO_4^{2-}	4.56	1.47	15.69	5.36	2.01	6.26	1.18
NH_4^+	1.32	0.47	4.53	1.20	0.88	1.40	0.91
Other Ions [e]	0.05	0.01	0.17	0.08	0.03	0.09	1.60
Others	15.86	5.65	54.53	65.87	38.43	76.97	4.15

[a] Conditions without Sand and Dust Storm (SDS) events were taken with respect to $PM_{10} < 50$ μg/m^3.
[b] Conditions with SDS events were taken with respect to $PM_{10} > 70$ μg/m^3.
[c] EC: elemental carbon.
[d] OC: elemental carbon.
[e] Other ions include F^-, NO_2^-, Br^-, and PO_4^{3-}.

4. Discussion

4.1. Compliance with WHO and Jordanian air quality standards

A detailed literature review of PM concentrations and their chemical speciation in different regions of the world can be found in Table S1 and Table S2.

The Jordanian standards (JS-1140/2006) sets the annual limit for PM_{10} and $PM_{2.5}$ as 70 μg/m^3 and 15 μg/m^3; respectively. Accordingly, the reported mean annual PM_{10} was below its limit value, but the annual $PM_{2.5}$ was three times higher than its limit value. Following the 24-h mean limit value, PM_{10} and $PM_{2.5}$ have limit values of 120 μg/m^3 and 65 μg/m^3, respectively. Here, the daily mean PM_{10} exceeded the limit values six times, and the $PM_{2.5}$ exceedance occurred seven times. These exceedances were during the SDS events. The World Health Organization's (WHO) previous air quality guidelines in 2005 for PM_{10} recommended that the annual and 24h average not to exceed 20 μg/m^3 and 50 μg/m^3, respectively. And that for the $PM_{2.5}$ annual and 24h average not to exceed 10 μg/m^3 and 25 μg/m^3; respectively. Accordingly, the observed annual PM_{10} and $PM_{2.5}$ here exceeded the annual WHO limit value. As for the 24h mean, only six days did not exceed their $PM_{2.5}$ limit value and twenty-five days did not exceed their PM_{10} limit value.

The WHO published an update on global air quality during 2008–2016 (World Health Organisation, 2018). According to that database, the world's overall annual mean PM_{10} was ~72 μg/m^3 during 2008–2016, which is slightly higher than what was observed during our measurement campaign. Compared to Jordanian cities reported in that database, the annual mean PM_{10} and $PM_{2.5}$ for Al-Zarqa', Amman, and Irbid in 2017 was 82, 68, and 53 μg/m^3; respectively. These are in accordance with our observation here. Compared to countries around the Mediterranean Sea in 2016, the annual mean PM_{10} in Jordan was higher than reported in the WHO database in urban, suburban, and residential sites. For example, the annual mean PM_{10} in Cyprus (4 sites) was 37 ± 6 μg/m^3 (range 29–41 μg/m^3), Greece (12 sites) was 52 ± 18 μg/m^3 (range 21–43 μg/m^3), Turkey (80 sites) was 52 ± 18 μg/m^3 (range 17–91 μg/m^3), Italy (231 sites) was about 25 ± 6 μg/m^3 (range 10–43 μg/m^3), and Malta (2 sites) was 38 ± 8 μg/m^3 (range 32–43 μg/m^3). And compared to other cities in the Middle East as reported by the WHO database, the annual mean PM_{10} in Jordan was lower than what was observed in Egypt (249–284 μg/m^3; two sites), Kuwait (130 ± 35 μg/m^3; 9 sites), and the United Arab of Emirates (122–153 μg/m^3; three sites).

4.2. Comparison with previous observations worldwide

With respect to previous $PM_{2.5}$ observations in the region, the reported values in this study remain within the range (22–66 μg/m^3) as compared to East Jerusalem (Palestine (von Schneidemesser et al., 2010)), Beirut (Lebanon (Fadel et al., 2023; Fakhri et al., 2023; Waked et al., 2013)), Riyadh (Saudi Arabia (Bian et al., 2018)), Kuwait (Kuwait (Brown et al., 2008)), Doha (Qatar (Javed and Guo, 2021)), and Busher and Tehran (Iran (Arfaeinia et al., 2016; F.F. Ghasemi et al., 2023a,b)) in addition, Amman (Jordan (von Schneidemesser et al., 2010)).

The concentrations in Jordan and its neighboring countries are higher than those observed around the Mediterranean EU countries (Turkey, Greece, Italy, and Spain), with a range 11–30 μg/m^3 (Cesari et al., 2018; Grivas et al., 2012; Mertoglu et al., 2022; Paraskevopoulou et al., 2015; Siciliano et al., 2018; Sillanpää et al., 2005; Tolis et al., 2014; Viana et al., 2006, 2007b) and other Eu countries (Portugal, France, Belgium, Germany, Netherland, Czech Republic, Poland, and Finland) with a range 8–34 μg/m^3 (Bencs et al., 2008; Juda-Rezler et al., 2020; Moufarrej et al., 2020; Pio et al., 2020; Schwarz et al., 2019; Sillanpää et al., 2005; Viana et al., 2007b). Also, in the USA and South Korea, the $PM_{2.5}$ concentrations reported were lower than what was observed in this study (Blanchard et al., 2008; Kim et al., 1999; Shon et al., 2013). In Chinese and Indian cities, $PM_{2.5}$ remains to be at a record high compared to other regions in the world, with a range 30–200 μg/m^3 and 50–310 μg/m^3; respectively (Das et al., 2015; Devi et al., 2020; He et al., 2001; Mahapatra et al., 2021, 2018; Niu et al., 2022; Panda et al., 2023; Pipal et al., 2016; Sharma et al., 2016; Su et al., 2021; Tao et al., 2014; Wang et al., 2005, 2022; Zhang et al., 2011; Zhang et al., 2021a,b;

Zhou et al., 2016a,b).

As can be recalled from Table S1, the $PM_{2.5}$ OC and EC concentrations within the fine fraction ($PM_{2.5}$) reported in this study were smaller than those reported in the regions Palestine, Lebanon, Kuwait, Qatar, and Iran that were in the range EC (1.8–2.6 μg/m^3) and OC (1.8–15.4 μg/m^3) (Arfaeinia et al., 2016; Brown et al., 2008; Javed and Guo, 2021; von Schneidemesser et al., 2010; Waked et al., 2013). Our values were within the range observed in European cities: EC (0.4–6.6 μg/m^3) and OC (2.1–14.8 μg/m^3) (Cesari et al., 2018; Grivas et al., 2012; Juda-Rezler et al., 2020; Paraskevopoulou et al., 2015; Pio et al., 2020; Schwarz et al., 2019; Siciliano et al., 2018; Sillanpää et al., 2005; Viana et al., 2006, 2007b). Again, Chinese and Indian cities recorded higher concentrations of OC (12–31 μg/m^3) and EC (2.7–17.9 μg/m^3) than the values reported in this study (Devi et al., 2020; He et al., 2001; Mahapatra et al., 2021; Niu et al., 2022; Pipal et al., 2016; Sharma et al., 2016; Tao et al., 2014; Wang et al., 2022; Zhang et al., 2021a,b; Zhou et al., 2016a,b).

In comparison to other cities in the region, the $PM_{2.5}$ SI concentrations reported in this study is less than those observed in Qatar ($NO_3^- =$ 1.5 μg/m^3 and $SO_4^{2-} =$ 14.2 μg/m^3) and Iran (2.1, 3.9, and 6.8 respectively for Cl^-, NO_3^- and SO_4^{2-}) (Ghasemi et al., 2023a,b; Javed and Guo, 2021); see Table S1. The concentrations of Cl^-, NO_3^- and NH_4^+ reported in this study are within the range reported (0.03–0.94, 0.04–8.7, and 0.08–4.94 μg/m^{3,} respectively for Cl^-, NO_3^- and NH_4^+) in other cities in the EU but the concentration of SO_4^{2-} (0.23–3.89 μg/m^3) was slightly higher (Bencs et al., 2008; Cesari et al., 2018; Grivas et al., 2012; Juda-Rezler et al., 2020; Mertoglu et al., 2022; Moufarrej et al., 2020; Paraskevopoulou et al., 2015; Pio et al., 2020; Schwarz et al., 2019; Sillanpää et al., 2005; Tolis et al., 2014). However, the $PM_{2.5}$ SI is significantly higher in Indian and Chinese cities (Devi et al., 2020; Mahapatra et al., 2021; Niu et al., 2022; Panda et al., 2023; Sharma et al., 2016; Su et al., 2021; Tao et al., 2014; Verma et al., 2010; Wang et al., 2005, 2022; Zhang et al., 2021a,b; Zhang et al., 2011; Zhou et al., 2016a,b); see Table S1.

4.3. Warm versus cold conditions and SDS versus nonSDS events

The high concentrations of the carbonaceous and water-soluble ions during cold conditions (i.e. winter) were also reported in other urban environments in India and China (Niu et al., 2022; Sharma et al., 2016; Su et al., 2021; Zhou et al., 2016a,b). It is very well known that during cold conditions, the boundary layer height is lower than during warm conditions. Recalling this fact, it is most likely leading to two probable reasons: (1) the formation/emission of EC, Cl-, NO3-, and NH4+ is enhanced, or (2) the chemical reactions removing these components from the atmosphere are reduced. The speculation remains uncertain regarding the unchanged concentration for OC, SO_4^{2-}, F^-, NO_2^-, Br^-, and PO_4^{3-} between warm and cold conditions.

Similar results were reported in Qatar with respect to increased concentrations of carbonaceous and some water-soluble ions (namely NH_4^+ and SO_4^{2-}) during SDS (Javed and Guo, 2021). In that study, the PM_{10} concentration was around 120 μg/m^3 during SDS versus 200 μg/m^3. The corresponding increase was from 6 μg/m^3 to 12 μg/m^3 for OC, from 3 μg/m^3 to 4 μg/m^3 for EC, from 7 μg/m^3 to 10 μg/m^3 for NH_4^+, and from 19 μg/m^3 to 22 μg/m^3 for SO_4^{2-}.

4.4. General discussion on aerosol chemical composition

The carbonaceous (OC and EC) and water-soluble ions (TI) fractions in the PM fractions were inversely proportional to the PM concentrations (Fig. 5). The fraction decrement rate of the TI/PM was more than that of the OC/PM and EC/PM. The secondary versus primary sources in the urban atmosphere of Amman can be revealed from the correlation and the regression between OC and EC (Fig. 6). The correlation between EC and OC was around 0.6 for both $PM_{2.5}$ and PM_{10}. This can be considered as an intermediate correlation indicating that the carbonaceous aerosols in Amman come equally from primary and secondary sources. The y-intercept of the regression line (OC = m EC + b) represents the contribution from non-combustion sources of OC, such as road pavement dust. An intercept value of about 3 μg/m^3 indicates about 50% of the OC came from non-combustion sources.

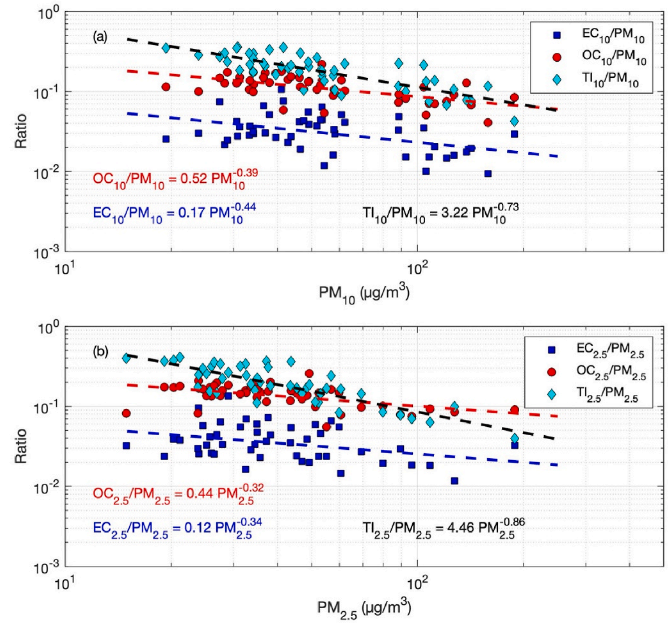

Fig. 5. The ratio of the chemical species to their corresponding particulate matter (a) PM_{10} and (b) $PM_{2.5}$.

The contribution of traffic emissions with respect to stationary sources is illustrated in Fig. 7a–b. Since the slope of the regression line ($SO_4^{2-} =$ m NO_3^- + b) is less than one, which indicates traffic emissions dominate the PM in the urban atmosphere of Amman.

The contribution of agricultural sources in Amman urban atmosphere is very weak because the regression line ($NH_4^+ =$ m NO_3^- + b) has a low regression slope of about 0.3 for $PM_{2.5}$ and almost negligible for PM_{10} (Fig. 7c–d).

Finally, the regression analysis suggests complete neutralization of $SO_4^{2-}$by NH_4^+ because the slope ($SO_4^{2-} =$ m NH_4^+ + b) was about 1.6 for $PM_{2.5}$ (Fig. 7e–f). However, additional reactions could be involved in the PM_{10} samples because the slope for the PM_{10} (about 1.2) was less than that for the $PM_{2.5}$. The complete neutralization suggests that $(NH_4)_2SO_4$, was the major species formed by $SO_4^{2-}$and NH_4^+ instead of NH_4HSO_4.

High EC and some water-soluble ions (Cl^-, NO_3^-, and NH_4^+) concentrations in winter can be related to a less developed boundary layer, which tends to be shallower in the winter (cold conditions) than in the summer. High concentrations of NO_3^- and NH_4^+ can be related to the thermal instability of NH_4NO_3 (volatile at relatively high temperatures); NO_3^- may react with coarse $CaCO_3$ and NaCl; forming coarse Na–$CaNO_3$. High concentrations of Cl^- can be linked to higher impact of marine air masses.

5. Conclusions

The Eastern Mediterranean is a unique region for air pollution because it is the junction point between three continents, exchanging air pollution transported between Africa, Asia, and Europe. In this study, we investigated, for the first time, the concentrations of carbonaceous aerosols (elemental carbon (EC) and organic carbon (OC)) and water-soluble ions (WSIIs) as observed in $PM_{2.5}$ and PM_{10} collected during 11 months at an urban site in Amman, Jordan.

The $PM_{2.5}$ total carbon (TC) annual mean was 7.6 ± 3.6 μg/m^3, which accounted for 16.3% of the $PM_{2.5}$. The corresponding $PM_{2.5}$ OC

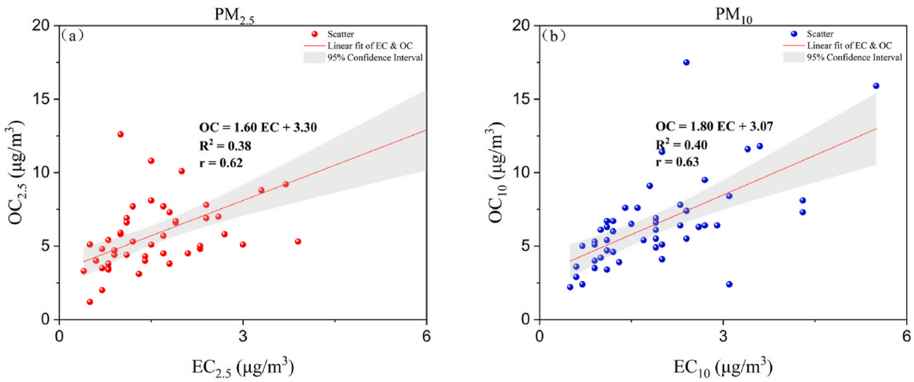

Fig. 6. Regression relationship between OC and EC in the PM observed in the urban atmosphere of Amman.

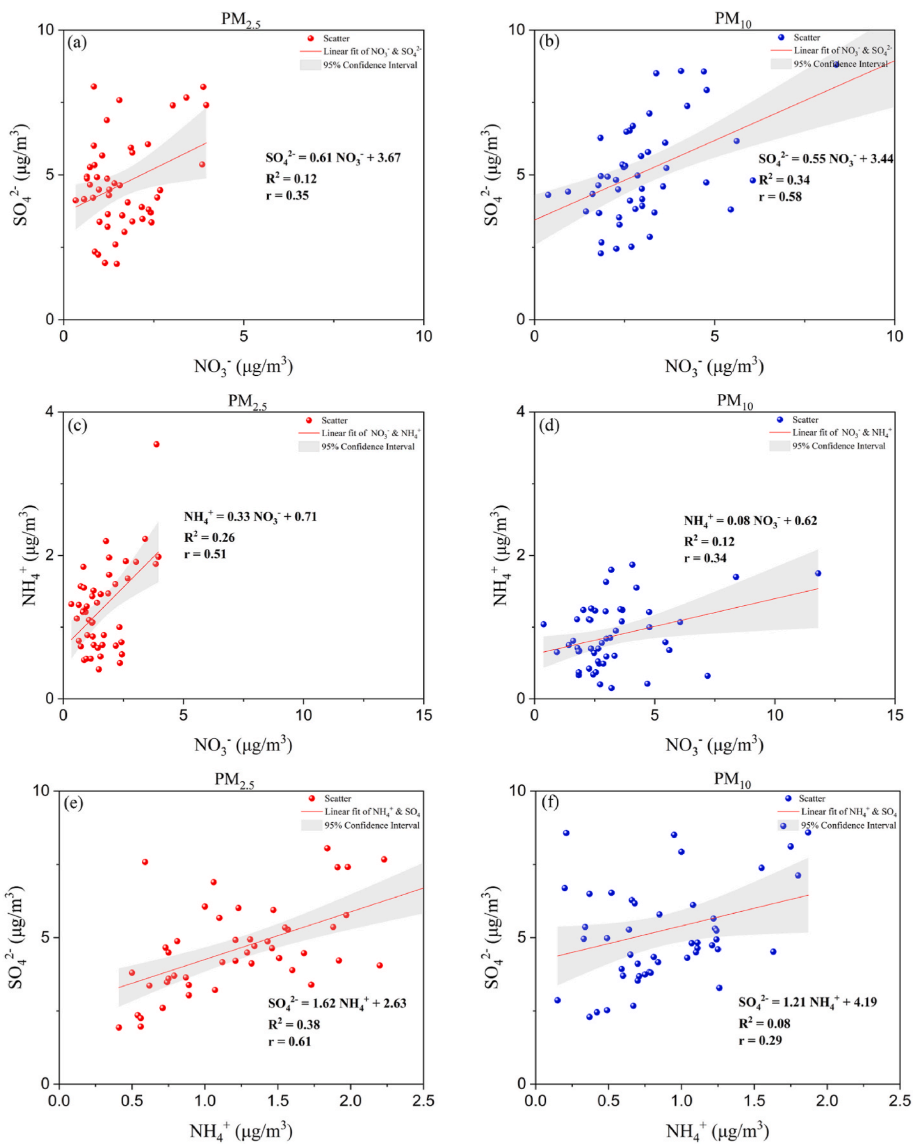

Fig. 7. Regression relationship between different ions (a–b) SO_4^{2-} versus NO_3^-, (c–d) NH_4^+ versus NO_3^-, (e–f) SO_4^{2-} versus NH_4^+ in the $PM_{2.5}$ (left panel) and PM_{10} (right panel).

and EC concentrations were 5.9 ± 2.8 μg/m^3 and 1.7 ± 1.1 μg/m^3; respectively. The PM_{10} TC annual mean was 8.4 ± 3.9 μg/m^3, which accounted 13.3%. The corresponding PM_{10} OC and EC were 6.5 ± 3.1 μg/m^3 and 11.9 ± 1.1 μg/m^3, respectively.

The $PM_{2.5}$ total water-soluble ions (TI) annual mean was 7.9 ± 1.9 μg/m^3, which accounted to about 16.9%. The PM_{10} was 10.1 ± 2.8 μg/m^{3,} accounting for about 16.0%. The minor ions (F^-, NO_2^-, Br^-, and PO_4^{3-}) constituted less than 1% in the PM fractions. The major fraction was for SO_4^{2-} with an average 4.7 ± 1.6 μg/m^3 (10.0%) as $PM_{2.5}$ and 5.3 ± 1.9 μg/m^3 (8.3%) as PM_{10}. The SO_4^{2-} fraction of $PM_{2.5}$ (10%) was larger than PM_{10} (8%), indicating that it is mainly emitted within the fine fraction. NH_4^+ had higher amounts as $PM_{2.5}$ (1.3 ± 0.6 μg/m^3; 2.7%) than that in PM_{10} (0.9 ± 0.4 μg/m^3; 1.4%).

During sand and dust storm (SDS) events, TC, Cl^-, and NO_3^- were doubled in both $PM_{2.5}$ and PM_{10}, SO_4^{2-} did not increase significantly, and NH_4^+ slightly decreased. Afterall, more extensive long-term measurements and monitoring are needed in this region to include an advanced chemical and physical characterization for urban aerosols.

Regression analysis revealed that carbonaceous aerosols in Amman's urban atmosphere came equally from primary and secondary sources and about 50% of the OC came from non-combustion sources. Furthermore, traffic emissions dominated the $PM_{2.5,}$ and agricultural sources had negligible effect. It is clear that SO_4^{2-} was completely neutralized by NH_4^+ in the $PM_{2.5}$ but there could be additional reactions involved in the PM_{10}. As such, $(NH_4)_2SO_4$, was the significant species formed by SO_4^{2-} and NH_4^+ instead of NH_4HSO_4.

After all, further monitoring and long-term sample collection are needed to quantify ions, anions, carbonaceous, and elemental speciation. This will provide an insight into the source apportionment of aerosols in the urban atmosphere of Amman, Jordan.

CRediT authorship contribution statement

Afnan Al-Hunaiti: Writing – review & editing, Writing – original draft, Visualization, Supervision, Resources, Project administration, Methodology, Investigation, Funding acquisition, Formal analysis, Data curation, Conceptualization. **Zaid Bakri:** Writing – review & editing, Validation, Software, Formal analysis. **Xinyang Li:** Writing – review & editing, Formal analysis. **Lian Duan:** Writing – review & editing, Visualization, Formal analysis. **Asal Al-Abdallat:** Writing – review & editing, Formal analysis. **Andres Alastuey:** Writing – review & editing, Validation, Formal analysis. **Mar Viana:** Writing – review & editing, Validation, Resources, Methodology, Investigation, Formal analysis, Data curation, Conceptualization. **Sharif Arar:** Writing – review & editing. **Tuukka Petäjä:** Writing – review & editing. **Tareq Hussein:** Writing – review & editing, Writing – original draft, Visualization, Validation, Supervision, Software, Resources, Project administration, Methodology, Investigation, Funding acquisition, Formal analysis, Data curation, Conceptualization.

Informed consent statement

Not applicable.

Institutional review board statement

Not applicable.

Funding

This research was funded by the Deanship of Scientific Research (DSR, project number 2015) at the University of Jordan. Academy of FinlandCenter of Excellence (project No. 272041). eCOST action (inDUST, project number CA16202) support via the Short-Term Scientific Mission (STSM) mobility grant.

Declaration of competing interest

The authors declare that they have no known competing financial interests or personal relationships that could have appeared to influence the work reported in this paper.

Acknowledgments

This research was part of a close collaboration between the University of Jordan, the Institute of Environmental Assessment and Water Research (IDAEA-CSIC), and the Institute for Atmospheric and Earth System Research (INAR/Physics, University of Helsinki). We acknowledge the financial support provided by the Deanship of Scientific Research (DSR, project No. 2015; University of Jordan), Academy of Finland via the Atmosphere and Climate Competence Center (ACCC, project No. 272041) Flagship, and the Eastern Mediterranean and Middle East Climate and Atmosphere Research (EMME-CARE, EU Horizon 2020 RI, project No. 856612). The work was supported by the Spanish Ministry of Science and Innovation (Project CEX2018-000794-S) and by AGAUR (project 2017 SGR41). Open access funding was provided by the University of Helsinki. This manuscript was written and completed during the research visit of the first author (Afnan Al-Hunaiti) that was spent at the Aalto University and supported by the University of Jordan during 2024.

Appendix A. Supplementary data

Supplementary data to this article can be found online at https://doi.org/10.1016/j.pce.2024.103783.

Table S1
$PM_{2.5}$ concentrations and corresponding carbonaceous (OC and EC) and some water-soluble ions (SI) concentrations reported in selected previous studies and investigations.

Location	Year	Background	$PM_{2.5}$	$OC_{2.5}$	$EC_{2.5}$	Cl^-	NO_3^-	NH_4^+	SO_4^{2-}	References
Jordan, Amman	2007	Residence and commerce	40 ± 9	6.7 ± 0.5	2.6 ± 0.8	–	–	–	–	(von Schneidemesser et al., 2010)
Palestine, East Jerusalem	2007	Residence and commerce	27 ± 10	5.6 ± 1.4	2.2 ± 0.5	–	–	–	–	(von Schneidemesser et al., 2010)
Lebanon, Beirut	2011	Urban	21.9	5.6	1.8	–	–	–	–	(Waked et al., 2013)
Lebanon, Beirut	April–October 2014	Urban	29 ± 16	4.4 ± 1.6	1.0 ± 0.5	0.3 ± 0.6	0.9 ± 0.9	1.4 ± 0.6	8.9 ± 4.4	(Fakhri et al., 2023)
		Semi-urban USJ	32 ± 14	4.6 ± 1.8	0.9 ± 0.6	0.3 ± 0.5	0.7 ± 0.6	1.2 ± 0.6	8.1 ± 3.7	
Lebanon, Beirut	December 2018–October 2019	Urban	33.6 (4.1–145)	4.6 (1.3–11.9)	1.3 (0.3–4.4)	0.58 (<4.7)	1.6 (0.1–8.0)	1.8 (0.1–5.4)	5.6 (0.9–15.3)	(Fadel et al., 2023)
		Urban	26.0 (3.9–96)	3.0 (0.5–8.9)	0.5 (0.1–1.8)	0.22 (<3.6)	1.1 (<7.3)	1.9 (0.1–5.0)	5.7 (0.9–13.6)	

(continued on next page)

Table S1 (*continued*)

Location	Year	Background	$PM_{2.5}$	$OC_{2.5}$	$EC_{2.5}$	Cl^-	NO_3^-	NH_4^+	SO_4^{2-}	References
Saudi Arabia, Riyadh	2012	Urban	–	4.7 ± 4.4	2.1 ± 2.5	–	–	–	–	(Bian et al., 2018)
Kuwait, Kuwait	2004–2005	Residence	30.8 ± 16.6	3.4 ± 1.4	1.9 ± 0.9	–	–	–	–	(Brown et al., 2008)
Qatar, Doha	May–December 2015	Urban Overall	39.81 ± 14.00	1.79 ± 1.13	2.63 ± 1.11	–	1.51 ± 1.20	–	14.16 ± 8.74	(Javed and Guo, 2021)
		SDS	53.06 ± 8.90	2.79 ± 1.48	2.85 ± 1.22	–	1.82 ± 0.68	–	13.08 ± 4.62	
		Non SDS	36.29 ± 14 0.00	1.55 ± 0.88	2.58 ± 1.08	–	1.43 ± 1.28	–	14.45 ± 9.49	
Iran, Busher	December 2016–September 2017	Industrial and Urban	65.77 ± 49.84	–	–	2.06 ± 1.21	3.88 ± 3.70	–	6.76 ± 4.63	(Ghasemi et al., 2023)
Iran, Tehran	2013–2014	Urban	41.19	15.35 ± 6.05	2.25 ± 0.65	–	–	–	–	(Arfaeinia et al., 2016)
Turkey, Istanbul	January 2017–January 2018	Urban	–	–	–	–	0.042	0.076	0.228	(Mertoglu et al., 2022)
Greece, Kozani	December	Urban		–	–			–		(Tolis et al., 2014)
	2009–January 2010	Warm	25.75 ± 11.19			0.03	0.78		3.89	
	July 2010	Cold	14.68 ± 8.39			0.07	1.41		2.25	
Greece, Athens	2008–2013		20 ± 11	2.1 ± 1.3	0.54 ± 0.39	–	0.45 ± 0.19	0.67 ± 0.26	3.1 ± 0.8	(Paraskevopoulou et al., 2015)
Greece, Athens	2003	Urban	–	6.8	2.2	–	–	–	–	(Grivas et al., 2012)
Greece, Athens	June–July 2003	Urban, summer	25.3	6.6	1.7	–	–	–	–	(Sillanpää et al., 2005)
Italy, Apulia region	2015	Costal rural	11 ± 6	3.5 ± 2.8	0.35 ± 0.18	–	–	–	–	(Siciliano et al., 2018)
Italy	2012–2013	Veneto Province	–	5.5	1.3	–	–	–	–	(Khan et al., 2016)
Italy, Lecce	July 2013–July 2014	Urban Overall	18.7 ± 11.3	5.4 ± 4.8	0.6 ± 0.4	0.17 ± 0.21	0.77 ± 1.15	–	2.61 ± 1.78	(Cesari et al., 2018)
		Warm	15.2 ± 6.4	3.0 ± 1.7	0.4 ± 0.2	0.08 ± 0.13	0.33 ± 0.17		3.11 ± 2.06	
		Cold	22.5 ± 14.0	7.3 ± 6.0	0.8 ± 0.5	0.26 ± 0.24	1.22 ± 1.51		2.05 ± 1.19	
Spain, Barcelona	November–December	Urban								(Viana et al., 2007)
	2004	Winter	29.1 ± 15.3	6.9 ± 2.5	2.6 ± 1.4	–	–	–	–	
	July–August 2004	Summer	17.7 ± 6.0	3.6 ± 1.4	1.5 ± 0.7	–	–	–	–	
Spain, Barcelona	2004	Urban	16.4–17.7	3–4 (summer)	1–2 (summer)	–	–	–	–	(Viana et al., 2006)
Spain, Barcelona	March–May 2003	Urban, spring	20.0	3.2	1.5	–	–	–	–	(Sillanpää et al., 2005)
Portogal, Porto	2013–2014	Urban, Overall	25.8 ± 15.2	5.86 ± 4.79	4.80 ± 3.04	0.55 ± 0.68	1.07 ± 1.00	0.61 ± 0.69	2.10 ± 1.95	(Pio et al., 2020)
		Summer	28.8 ± 16.6	5.96 ± 4.57	4.21 ± 2.69	0.22 ± 0.23	0.81 ± 0.68	0.82 ± 0.89	3.17 ± 2.54	
		Winter	28.8 ± 6.2	8.34 ± 6.14	6.58 ± 0.59	0.94 ± 0.93	1.64 ± 1.32	0.53 ± 0.41	1.14 ± 0.48	
France, Dunkerque	2010–2011	Urban, Industrial Winter and spring	29.2 ± 24.4	–	–	0.7 ± 0.4	8.7 ± 10.7	2.0 ± 1.3	2.8 ± 2.0	(Moufarrej et al., 2020)
Belgium, Ghent	January–February	Urban								(Viana et al., 2007)
	2005	Winter	20.8 ± 18.3	5.4 ± 4.5	1.2 ± 0.6	–	–	–	–	
	June–July 2004	Summer	15.7 ± 4.9	2.7 ± 1.0	0.8 ± 0.3	–	–	–	–	
Belgium, Flanders	September	Rural	11–45	–	–	0.09–0.20	0.34–6.53	1.31–3.54	0.79–3.26	(Bencs et al., 2008)
	2001–April 2003	Suburban				0.07–0.35	0.40–3.60	0.89–2.62	0.43–4.48	
		Urban				0.10–0.19	3.22–7.63	2.40–4.94	4.23–4.30	
		Industrial				0.07–0.12	0.76–3.15	1.74–2.48	2.69–4.12	
Netherland, Amsterdam	January–February	Urban								(Viana et al., 2007)
	2006	Winter	34.4 ± 15.8	6.7 ± 3.8	1.7 ± 0.9	–	–	–	–	
	July–August 005	Summer	17.8 ± 7.8	3.9 ± 1.6	1.9 ± 0.7	–	–	–	–	
Netherland, Amsterdam	January–March 2003	Urban, winter	25.4	6.0	1.4	–	–	–	–	(Sillanpää et al., 2005)
Germany, Duisburg	October–November 2002	Urban, autumn	14.7	3.5	1.3	–	–	–	–	(Sillanpää et al., 2005)
Czech Republic, Prague	November 2002–January 2003	Residential, winter	29.6	14.8	1.7	–	–	–	–	(Sillanpää et al., 2005)
Czech Republic, Prague	April 2008–March 2009	Suburban								(Schwarz et al., 2019)
		Libuš	24.4 ± 13.0	5.09	1.29	0.13	2.36	1.77	2.63	
		Suchdol	25.1 ± 22.1	5.22	10.53	0.14	2.62	0.14	3.14	
Poland, Warsaw	2016	Urban	18.8 ± 11.9	5.56	1.47	–	2.44	1.17	2.17	(Juda-Rezler et al., 2020)
	Winter		27.5	8.33	1.91	–	4.25	1.74	2.73	
	Spring		2.0.6	5.62	1.57	–	2.54	1.58	2.20	
	Summer		11.5	3.79	0.12	–	0.53	0.50	1.77	
	Autumn		15.7	4.27	1.23	–	2.40	0.77	1.95	
Finland, Helsinki	March–May 2003	Urban, spring	8.3	2.8	0.7	–	–	–	–	(Sillanpää et al., 2005)
USA, Seattle	1996–1999	Urban	8.9 ± 7.5	2.2 (modeled)	0.852 (modeled)	–	–	–	–	(Maykut et al., 2003)

(*continued on next page*)

Table S1 (*continued*)

Location	Year	Background	$PM_{2.5}$	$OC_{2.5}$	$EC_{2.5}$	Cl^-	NO_3^-	NH_4^+	SO_4^{2-}	References
USA	2001–2004									(Blanchard et al., 2008)
Birmingham		Urban	17.1	4.3	1.8	–	1.0	2.1	4.4	
Atlanta		Urban	16.1	4.2	1.4	–	0.9	2.2	4.6	
Centreville		Rural	12.0	2.8	0.5	–	0.4	1.2	3.7	
Yorkville		Rural	13.2	2.7	0.6	–	0.8	2.4	4.4	
Gulfport		Urban	11.0	2.1	0.6	–	0.4	1.2	3.4	
Pensacola		Urban	12.5	2.8	0.8	–	0.4	1.3	3.4	
Oak Grove		Rural	11.4	2.6	0.5	–	0.3	1.0	3.4	
Brazil, Rondonia	2002		–	19.5–86.4	0.6–3.6	–	2.1 ± 1.4	1.26 ± 0.51	2.7 ± 0.3	(Kundu et al., 2010)
Australia, Brisbane	October 2010–August 2012	Urban overall	–	2.6	0.6	–	–	–	–	(Crilley et al., 2016)
		Summer		2.69 ± 0.86	0.46 ± 0.22					
		Winter		2.36 ± 1.11	0.68 ± 0.45					
Japan, Nagoya	2003–2019	Residence	–	3.3	0.7	–	–	–	–	(Yamagami et al., 2021)
South Korea, Seoul	1997	Urban	–	2.97	0.32	–	–	–	–	(Kim et al., 1999)
South Korea, Seoul	2010		25.2 ± 19.0	–	–	0.49 ± 0.64	12.3 ± 7.17	3.73 ± 3.59	5.19 ± 4.58	(Shon et al., 2013)
China, Beijing	2000	Urban and residence	127	29.1	10.1	–	–	–	–	(He et al., 2001)
China, Chegongzhuang	2000	Urban and residence	115	21.5	8.7	–	–	–	–	(He et al., 2001)
China, Beijing	2001–2003		154.3 ± 145.7	–	–	–	11.52 ± 11.37	8.72 ± 7.66	17.07 ± 16.52	(Wang et al., 2005)
China, Xi'an	2006–2007		194.1 ± 78.6	–	–	3.07 ± 3.13	16.4 ± 10.1	11.4 ± 6.8	35.6 ± 19.5	(Zhang et al., 2011)
China, Chengdu	2011		119 ± 56	17 ± 8	7 ± 4	–	10.7 ± 7.8	11.6 ± 7.3	25.0 ± 14.1	(Tao et al., 2014)
China, Shanghai	2011	Spring	55 ± 35	9.72 ± 4.95	2.35 ± 1.64	3.50 ± 1.60	12.07 ± 9.93	6.53 ± 5.73	11.29 ± 7.71	(M. Zhou et al., 2016)
		Summer	34 ± 26	9.10 ± 6.51	2.06 ± 1.52	2.21 ± 1.20	6.43 ± 7.58	5.41 ± 4.75	9.54 ± 6.99	
		Fall	40 ± 39	8.27 ± 6.95	1.93 ± 1.56	1.20 ± 1.28	7.67 ± 10.66	5.62 ± 6.26	9.67 ± 8.78	
		Winter	65 ± 55	11.18 ± 7.24	2.43 ± 2.01	4.21 ± 6.21	13.33 ± 11.23	8.11 ± 6.05	11.70 ± 10.16	
China	Nov 2012–Jul 2013	Urban								(J. Zhou et al., 2016)
Wuqing, Tianjin			148.9 ± 91.1	14.1 ± 13.8	1.6 ± 0.5	6.0 ± 5.1	19.6 ± 16.5	8.5 ± 5.9	24.2 ± 21.8	
Haining, Zhejiang			109.6 ± 59.4	9.0 ± 3.7	1.4 ± 0.5	2.3 ± 1.8	13.9 ± 12.0	6.1 ± 4.3	16.5 ± 9.9	
Zhongshan, Guangdong			60.5 ± 46.5	7.0 ± 5.0	1.2 ± 0.6	1.2 ± 1.1	6.4 ± 7.7	2.8 ± 2.8	9.8 ± 6.3	
Deyang, Sichuan			121.5 ± 101.1	13.8 ± 13.2	1.4 ± 0.7	2.0 ± 2.0	10.2 ± 12.7	6.3 ± 6.4	21.6 ± 18.3	
China, Hangzhou	2016	Urban								(Niu et al., 2022)
		Winter	100.3	8.3	3.8	4.0 ± 2.8	24.0 ± 15.4	9.9 ± 5.1	16.7 ± 9.2	
		Summer	52.3	6.6	2.0	0.5 ± 0.3	3.2 ± 3.5	3.9 ± 2.3	7.1 ± 3.8	
China, Beijing	Apr 2016–Feb 2018	Urban								(Su et al., 2021)
		Spring	55.05	–	–	0.86	12.78	6.80	8.51	
		Summer	40.94	–	–	0.41	9.80	7.83	9.40	
		Autumn	50.39	–	–	1.12	19.12	8.21	5.99	
		Winter	35.01	–	–	1.61	6.75	3.42	4.14	
China, Tianjin	Oct 2017–Aug 2018	Urban	61.7 ± 37.7	6.9 ± 5.0	2.3 ± 1.8	1.6 ± 2.0	9.4 ± 11.8	6.6 ± 5.9	6.0 ± 4.7	(Zhang et al., 2021)
China, Hangzhou	2018	Urban								(Niu et al., 2022)
		Winter	65.6	7.2	1.9	1.6 ± 1.1	21.7 ± 17.2	10.5 ± 5.8	11.6 ± 7.8	
		Summer	29.7	9.7	1.7	0.3 ± 0.3	2.4 ± 0.1	0.9 ± 0.3	5.1 ± 3.8	
China, Jinan	May–Dec 2019	Industrial	53.4 ± 43.9	9.3 ± 5.5	2.2 ± 1.5	0.2 ± 0.1	14.6 ± 14.2	8.1 ± 6.8	9.1 ± 6.4	(Wang et al., 2022)
India, Bhubaneswar	August 2015–April 2016	Rural	50.2 ± 23.2	6.2	3.2	1.0	2.0	5.0	12.0	(Panda et al., 2023)
India, Bhubaneswar	November 2014–January 2015	Reference	107	13.5	8.8	1.1	6.1	8.9	19.5	(Mahapatra et al., 2021)
		Residential	101	16.3	11.1	1.2	3.0	8.0	18.5	
		Industrial	142	18.1	11.6	1.3	4.7	8.0	17.5	
		Traffic	129	14.2	12.1	1.3	5.9	8.5	18.2	
India, Bhubaneswar	January 2012–December 2014	Urban								(Mahapatra et al., 2018)
		Winter	55 ± 23.4	–	–	–	–	–	–	
		Pre monsoon	15.7 ± 6.2	–	–	–	–	–	–	
		Monsoon	25.3 ± 15.7	–	–	–	–	–	–	
		Post monsoon	27 ± 15.8	–	–	–	–	–	–	
India, Kolkata	2013–2014	Urban, Winter	313 ± 181	–	–	–	–	–	–	(Das et al., 2015)
India, Pune	May 2013–April 2014	–	109.6 ± 23.2	31.3 ± 7.4	4.2 ± 2.4					(Pipal et al., 2016)
India, Raipur	2005–2006	Overall	167.0 ± 75.3	–	–	–	8.2 ± 7.1	8.8 ± 7.7	46.5 ± 32.8	(Verma et al., 2010)
		Summer	239.0 ± 74.8							
		Fall	74.1 ± 23.0							
		Winter	110.3 ± 62.6							
		Spring	77.1 ± 50.0							
India, New Delhi	January 2013–December 2014	Overall	122 ± 94.1	17.9 ± 14.3	10.4 ± 8.04	7.77 ± 5.72	10.0 ± 9.82	9.40 ± 8.59	12.9 ± 8.08	(Sharma et al., 2016)
		Winter	216 ± 93.2	31.0 ± 15.0	17.9 ± 7.77	10.9 ± 6.68	18.9 ± 11.4	16.2 ± 10.4	16.9 ± 11.2	
		Summer	81.8 ± 24.9	11.4 ± 3.72	7.15 ± 3.05	5.64 ± 3.00	5.82 ± 2.03	8.34 ± 2.97	10.3 ± 3.85	

(continued on next page)

Table S1 (*continued*)

Location	Year	Background	$PM_{2.5}$	$OC_{2.5}$	$EC_{2.5}$	Cl^-	NO_3^-	NH_4^+	SO_4^{2-}	References
		Monsoon	67.9 ± 56.1	10.1 ± 9.10	5.58 ± 5.41	6.48 ± 5.19	4.18 ± 3.16	3.43 ± 3.75	11.3 ± 5.13	
India	May–June 2017	Residential								(Devi et al., 2020)
New Delhi			91.5	20.3	4.92	0.46	0.09	3.78	0.81	
Kanpur			83.2	20.3	3.82	0.22	0.05	4.41	1.16	
Prayagraj			66.0	13.5	2.65	0.11	0.05	3.1	0.86	
Varanasi			102	13.4	2.77	0.92	0.29	2.21	0.89	
Patna			77.4	30.2	6.1	0.1	0.1	2.4	1	
Bhagalpur			98.0	12	3.27	0.46	0.02	2.06	0.93	
Kolkata			93.2	15.8	6.43	0.36	0.21	5.85	0.96	

Table S2
PM_{10} concentrations and corresponding carbonaceous (OC and EC) and some water-soluble ions (SI) concentrations reported in selected previous studies and investigations.

Location	Year	Background	PM_{10}	OC_{10}	EC_{10}	Cl^-	NO_3^-	NH_4^+	SO_4^{2-}	References
Qatar, Doha	May–December 2015	Urban Overall	145.54	6.97	3.20	–	7.65	–	19.45	(Javed and Guo, 2021)
		SDS	198.15	12.12	3.80	–	9.64	–	21.87	
		Non SDS	119.21	5.70	3.06	–	7.15	–	18.88	
Saudi Arabia, Dammam	2016–2019	Industrial and Urban	177.4 ± 52.5	–	–	8.1 ± 2.6	10.3 ± 1.8	–	33.4 ± 4.6	(ElSharkawy and Ibrahim, 2019)
Spain, Barcelona	March–May 2003	Urban, spring	46.3	13.1	1.8	–	–	–	–	(Sillanpää et al., 2005)
Greece, Athens	June–July 2003	Urban, summer	54.0	30.6	2.0	–	–	–	–	(Sillanpää et al., 2005)
Greece, Kozani	December	Urban		–	–			–		(Tolis et al., 2014)
	2009–January 2010	Warm	35.29 ± 13.11			0.07	1.39		4.60	
	July 2010	Cold	19.62 ± 12.00			0.12	1.64		2.71	
Greece, Thessaloniki	2012	Urban	51.1 ± 14	11.3 ± 5.0	6.56 ± 2.14	–	–	–	–	(Samara et al., 2014)
Italy, Lecce	July 2013–July 2014	Urban Overall	29.5 ± 19.2	5.7 ± 5.0	0.8 ± 0.7	0.85 ± 1.40	1.48 ± 1.51	–	3.05 ± 1.93	(Cesari et al., 2018)
		Warm	24.8 ± 11.2	3.6 ± 2.0	0.5 ± 0.3	0.50 ± 1.07	1.05 ± 0.58		3.48 ± 2.08	
		Cold	34.7 ± 24.4	8.0 ± 6.1	1.1 ± 0.8	1.23 ± 1.60	1.93 ± 1.98		2.60 ± 1.67	
Italy, Apulia region	2015	Coastal rural	23 ± 14	5 ± 4	0.41 ± 0.19	–	–	–	–	(Siciliano et al., 2018)
Spain, Barcelona	2004	Urban	29.5 ± 8.5	4 (summer)	1 (summer)	–	–	–	–	(Viana et al., 2006)
Portogal, Porto	2013–2014	Urban, Overall	34.7	6.20	4.83	2.16	1.96	0.67	2.48	(Pio et al., 2020)
		Summer	37.4	6.41	4.25	1.16	1.97	0.85	3.73	
		Winter	36.6	8.62	6.62	2.54	2.17	0.54	1.30	
Netherland, Amsterdam	January–March 2003	Urban, winter	33.8	31.3	1.6	–	–	–	–	(Sillanpää et al., 2005)
Germany, Duisburg	October–November 2002	Urban, autumn	21.9	29.9	1.5	–	–	–	–	(Sillanpää et al., 2005)
Czeck Republi, Prague	November 2002–January 2003	Residential, winter	35.0	36.3	2.0	–	–	–	–	(Sillanpää et al., 2005)
Czech Republic, Prague	April 2008–March 2009	Suburban								(Schwarz et al., 2019)
		Libuš	26.68 ± 15.13	5.99 ± 6.24	1.59 ± 1.33	0.22 ± 0.38	3.15 ± 3.06	1.67 ± 1.52	2.86 ± 2.05	
		Suchdol	27.12 ± 23.24	6.53 ± 8.31	1.76 ± 1.80	0.25 ± 0.44	3.54 ± 3.06	0.14 ± 0.15	3.45 ± 3.34	
Czech Republic, Prague	–	Suburb	33 ± 23	5.5	0.74	–	–	–	–	(Vodička et al., 2013)
		Downtown	37 ± 22	4.8	0.8					
Hungary, Budapest	2002	Near-city	54	11	3.6	–	–	–	–	(Salma et al., 2004)
Finland, Helsinki	March–May 2003	Urban, spring	21.1	14.2	0.9	–	–	–	–	(Sillanpää et al., 2005)
Pakistan, Lahore	2010	Urban	406.2	63	21	–	–	–	–	(Alam et al., 2014)
India, Indo-Gangetic Plain	2015–2016	Residence	167 ± 45	44.3 ± 8.9 (Day)	–	–	–	–	–	(Arif et al., 2018)
India, Bhubaneswar	August 2015–April 2016	Rural	93.9 ± 47.8	–	–	–	–	–	–	(Panda et al., 2023)
India, Bhubaneswar	November 2014–January 2015	Rural	88.3 ± 30.6	–	–	–	–	–	–	(Mahapatra et al., 2021)
India, Bhubaneswar	January 2012–December 2014	Urban								(Mahapatra et al., 2018)
		Winter	147.3 ± 42.4	–	–	–	–	–	–	
		Pre monsoon	41.8 ± 15.3	–	–	–	–	–	–	
		Monsoon	78.6 ± 27.6	–	–	–	–	–	–	
		Post monsoon	85.47 ± 49.41	–	–	–	–	–	–	
India, Kolkata	2013–2014	Urban, Winter	445 ± 210	–	–	–	–	–	–	(Das et al., 2015)
India, Pune	May 2013–April 2014	–	166.9 ± 4	34.2 ± 6.2	5.0 ± 2.3					(Pipal et al., 2016)
India	May–June 2017	Residential								(Devi et al., 2020)
New Delhi			162	27.32	7.29	1.04	0.51	5.23	0.62	
Kanpur			147	33.27	6.40	0.83	0.09	6.34	0.80	
Prayagraj			118	18.56	5.81	1.01	0.07	5.49	0.81	

(*continued on next page*)

Table S2 (*continued*)

Location	Year	Background	PM_{10}	OC_{10}	EC_{10}	Cl^-	NO_3^-	NH_4^+	SO_4^{2-}	References
Varanasi			165	24.54	6.52	1.93	0.22	3.63	0.81	
Patna			149	36.1	6.61	0.32	0.33	3.34	0.79	
Bhagalpur			194	17.40	7.03	0.58	0.05	2.42	0.69	
Kolkata			151	25.6	7.32	1.03	0.08	8.61	0.67	
India, Indo-Gangetic Plain	2015–2016	Residence	283 ± 61	74.2 ± 14 (Night)	–	–	–	–	–	(Arif et al., 2018)
China, Taiyuan	2001–2002	Urban	146.36	25.89 (summer)	6.82 (summer)	–	–	–	–	(Tian et al., 2013)
South Korea, Seoul	1994	Urban	–	11.1	8.39	–	–	–	–	(Kim et al., 1999)
USA, Mira Loma	2001	Urban plume	–	15.91 ± 6.81	1.56 ± 0.56	–	–	–	–	Salmon et al. [76]

Data availability

Data will be made available on request.

References

Alam, K., Mukhtar, A., Shahid, I., Blaschke, T., Majid, H., Rahman, S., Khan, R., Rahman, N., 2014. Source apportionment and characterization of particulate matter (PM10) in urban environment of Lahore. Aerosol Air Qual. Res. 14. https://doi.org/10.4209/aaqr.2014.01.0005.

Al-Dousari, A.M., Ibrahim, M.I., Al-Dousari, N., Ahmed, M., Al-Awadhi, S., 2018. Pollen in aeolian dust with relation to allergy and asthma in Kuwait. Aerobiologia 34, 325–336. https://doi.org/10.1007/s10453-018-9516-8.

Arfaeinia, H., Hashemi, S.E., Alamolhoda, A.A., Kermani, M., 2016. Evaluation of organic carbon, elemental carbon, and water soluble organic carbon concentration in PM 2.5 in the ambient air of Sina Hospital district, Tehran, Iran Introduction 1. J Adv Environ Health Res.

Arif, M., Kumar, Rajesh, Kumar, Ramesh, Zusman, E., Singh, R.P., Gupta, A., 2018. Assessment of Indoor & Outdoor Black Carbon emissions in rural areas of Indo-Gangetic Plain: seasonal characteristics, source apportionment and radiative forcing. Atmos. Environ. 191. https://doi.org/10.1016/j.atmosenv.2018.07.057.

Behrooz, R.D., Esmaili-Sari, A., Bahramifar, N., Kaskaoutis, D.G., Saeb, K., Rajaei, F., 2017. Trace-element concentrations and water-soluble ions in size-segregated dust-borne and soil samples in Sistan, southeast Iran. Aeolian Res 25, 87–105. https://doi.org/10.1016/j.aeolia.2017.04.001.

Bencs, L., Ravindra, K., De Hoog, J., Rasoazanany, E.O., Deutsch, F., Bleux, N., Berghmans, P., Roekens, E., Krata, A., Van Grieken, R., 2008. Mass and ionic composition of atmospheric fine particles over Belgium and their relation with gaseous air pollutants. J. Environ. Monit. 10. https://doi.org/10.1039/b805157g.

Bian, Q., Alharbi, B., Shareef, M.M., Husain, T., Pasha, M.J., Atwood, S.A., Kreidenweis, S.M., 2018. Sources of PM2.5 carbonaceous aerosol in Riyadh, Saudi Arabia. Atmos. Chem. Phys. 18. https://doi.org/10.5194/acp-18-3969-2018.

Birch, M.E., Cary, R.A., 1996. Elemental carbon-based method for monitoring occupational exposures to particulate diesel exhaust. Aerosol. Sci. Technol. 25, 221–241. https://doi.org/10.1080/02786829608965393.

Blanchard, C.L., Hidy, G.M., Tanenbaum, S., Edgerton, E., Hartsell, B., Jansen, J., 2008. Carbon in southeastern U.S. aerosol particles: empirical estimates of secondary organic aerosol formation. Atmos. Environ. 42. https://doi.org/10.1016/j.atmosenv.2008.04.011.

Bozkurt, Z., 2018. Seasonal variation of water-soluble inorganic ions in PM_{10} in a city of northwestern Turkey. Environ. Forensics 19, 1–13. https://doi.org/10.1080/15275922.2017.1408159.

Brown, K.W., Bouhamra, W., Lamoureux, D.P., Evans, J.S., Koutrakis, P., 2008. Characterization of particulate matter for three sites in Kuwait. J. Air Waste Manage. Assoc. 58. https://doi.org/10.3155/1047-3289.58.8.994.

Cavalli, F., Viana, M., Yttri, K.E., Genberg, J., Putaud, J.-P., 2010. Toward a standardised thermal-optical protocol for measuring atmospheric organic and elemental carbon: the EUSAAR protocol. Atmos. Meas. Tech. 3, 79–89. https://doi.org/10.5194/amt-3-79-2010.

Cesari, D., De Benedetto, G.E., Bonasoni, P., Busetto, M., Dinoi, A., Merico, E., Chirizzi, D., Cristofanelli, P., Donateo, A., Grasso, F.M., Marinoni, A., Pennetta, A., Contini, D., 2018. Seasonal variability of PM2.5 and PM10 composition and sources in an urban background site in Southern Italy. Sci. Total Environ. 612. https://doi.org/10.1016/j.scitotenv.2017.08.230.

Cheng, B., Ma, Y., Li, H., Feng, F., Zhang, Y., Qin, P., 2022. Water-soluble ions and source apportionment of PM2.5 depending on synoptic weather patterns in an urban environment in spring dust season. Sci. Rep. 12. https://doi.org/10.1038/s41598-022-26615-y.

Crilley, L.R., Ayoko, G.A., Mazaheri, M., Morawska, L., 2016. Factors influencing the outdoor concentration of carbonaceous aerosols at urban schools in Brisbane, Australia: implications for children's exposure. Environ. Pollut. 208. https://doi.org/10.1016/j.envpol.2015.04.017.

Das, R., Khezri, B., Srivastava, B., Datta, S., Sikdar, P.K., Webster, R.D., Wang, X., 2015. Trace element composition of PM2.5 and PM10 from Kolkata–a heavily polluted indian metropolis. Atmos. Pollut. Res. 6. https://doi.org/10.5094/APR.2015.083.

Delfino, R.J., Sioutas, C., Malik, S., 2005. Potential role of ultrafine particles in associations between airborne particle mass and cardiovascular health. Environ. Health Perspect. 113, 934–946. https://doi.org/10.1289/ehp.7938.

Devi, N.L., Kumar, A., Yadav, I.C., 2020. PM10 and PM2.5 in Indo-Gangetic Plain (IGP) of India: chemical characterization, source analysis, and transport pathways. Urban Clim. 33. https://doi.org/10.1016/j.uclim.2020.100663.

Doronzo, D.M., Al-Dousari, A., Folch, A., Dagsson-Waldhauserova, P., 2016. Preface to the dust topical collection. Arabian J. Geosci. 9. https://doi.org/10.1007/s12517-016-2504-9.

ElSharkawy, M.F., Ibrahim, O.A., 2019. Sources and concentrations of acidic constituents in the ambient air of Saudi Arabia. Air Qual Atmos Health 12. https://doi.org/10.1007/s11869-019-00737-1.

Fadel, M., Courcot, D., Seigneur, M., Kfoury, A., Oikonomou, K., Sciare, J., Ledoux, F., Afif, C., 2023. Identification and apportionment of local and long-range sources of $PM_{2.5}$ in two East-Mediterranean sites. Atmos. Pollut. Res. 14. https://doi.org/10.1016/j.apr.2022.101622.

Fakhri, N., Fadel, M., Öztürk, F., Keleş, M., Iakovides, M., Pikridas, M., Abdallah, C., Karam, C., Sciare, J., Hayes, P.L., Hayes, P.L., Afif, C., 2023. Comprehensive chemical characterization of $PM_{2.5}$ in the large East Mediterranean-Middle East city of Beirut, Lebanon. J. Environ. Sci. (China) 133, 118–137. https://doi.org/10.1016/j.jes.2022.07.010.

Freyer, H.D., Kley, D., Volz-Thomas, A., Kobel, K., 1993. On the interaction of isotopic exchange processes with photochemical reactions in atmospheric oxides of nitrogen. J. Geophys. Res. 98. https://doi.org/10.1029/93jd00874.

Galindo, N., Yubero, E., Clemente, Á., Nicolás, J.F., Varea, M., Crespo, J., 2020. PM events and changes in the chemical composition of urban aerosols: a case study in the western Mediterranean. Chemosphere 244. https://doi.org/10.1016/j.chemosphere.2019.125520.

Ghasemi, F.F., Dobaradaran, S., Saeedi, R., Mohammadi, A., Darabi, A., Mahmoodi, M., 2023a. Outdoor $PM_{2.5}$ and their water-soluble ions in the Northern part of the Persian Gulf. Environmental Health Engineering and Management 10, 361–371. https://doi.org/10.34172/EHEM.2023.40.

Ghasemi, Fatemeh Faraji, Dobaradaran, S., Saeedi, R., Mohammadi, A., Darabi, A., Mahmoodi, M., 2023b. Outdoor PM2.5 and their water-soluble ions in the Northern part of the Persian Gulf. Environmental Health Engineering and Management 10. https://doi.org/10.34172/EHEM.2023.40.

Goudarzi, G., Shirmardi, M., Naimabadi, A., Ghadiri, A., Sajedifar, J., 2019. Chemical and organic characteristics of $PM_{2.5}$ particles and their in-vitro cytotoxic effects on lung cells: the Middle East dust storms in Ahvaz, Iran. Sci. Total Environ. 655, 434–445. https://doi.org/10.1016/j.scitotenv.2018.11.153.

Grivas, G., Cheristanidis, S., Chaloulakou, A., 2012. Elemental and organic carbon in the urban environment of Athens. Seasonal and diurnal variations and estimates of secondary organic carbon. Sci. Total Environ. 414. https://doi.org/10.1016/j.scitotenv.2011.10.058.

Gupta, L., Joshi, S., Habib, G., Sunder Raman, R., 2023. Characteristics and atmospheric processes of water-soluble ions in $PM_{2.5}$ and PM_{10} over an industrial city in the National Capital Region (NCR) of India. Atmos. Environ. 312. https://doi.org/10.1016/j.atmosenv.2023.120020.

He, K., Yang, F., Ma, Y., Zhang, Q., Yao, X., Chan, C.K., Cadle, S., Chan, T., Mulawa, P., 2001. The characteristics of PM2.5 in Beijing, China. Atmos. Environ. 35. https://doi.org/10.1016/S1352-2310(01)00301-6.

Hong, X., Yang, K., Liang, H., Shi, Y., 2022. Characteristics of water-soluble inorganic ions in $PM_{2.5}$in typical urban areas of Beijing, China. ACS Omega 7, 35575–35585. https://doi.org/10.1021/acsomega.2c02919.

Hussein, T., Li, X., Al-Dulaimi, Q., Daour, S., Atashi, N., Viana, M., Alastuey, A., Sogacheva, L., Arar, S., Al-Hunaiti, A., Petäjä, T., 2020. Particulate matter concentrations in a middle eastern city – an insight to sand and dust storm episodes. Aerosol Air Qual. Res. 20. https://doi.org/10.4209/aaqr.2020.05.0195.

Hussein, T., Li, X., Bakri, Z., Alastuey, A., Arar, S., Al-Hunaiti, A., Viana, M., Petäjä, T., 2022. Organic and elemental carbon in the urban background in an eastern mediterranean city. Atmosphere 13. https://doi.org/10.3390/atmos13020197.

Javed, W., Guo, B., 2021. Chemical characterization and source apportionment of fine and coarse atmospheric particulate matter in Doha, Qatar. Atmos. Pollut. Res. 12. https://doi.org/10.1016/j.apr.2020.10.015.

Juda-Rezler, K., Reizer, M., Maciejewska, K., Błaszczak, B., Klejnowski, K., 2020. Characterization of atmospheric PM2.5 sources at a Central European urban background site. Sci. Total Environ. 713. https://doi.org/10.1016/j.scitotenv.2020.136729.

Khan, M.B., Masiol, M., Formenton, G., Di Gilio, A., de Gennaro, G., Agostinelli, C., Pavoni, B., 2016. Carbonaceous PM2.5 and secondary organic aerosol across the Veneto region (NE Italy). Sci. Total Environ. 542. https://doi.org/10.1016/j.scitotenv.2015.10.103.

Khan, MdF., Shirasuna, Y., Hirano, K., Masunaga, S., 2010. Characterization of $PM_{2.5}$, $PM_{2.5\text{-}10}$ and $PM_{>10}$ in ambient air, Yokohama, Japan. Atmos. Res. 96, 159–172. https://doi.org/10.1016/j.atmosres.2009.12.009.

Kim, Y.P., Moon, K.C., Lee, J.H., Baik, N.J., 1999. Concentrations of carbonaceous species in particles at seoul and cheju in Korea. Atmos. Environ. 33. https://doi.org/10.1016/S1352-2310(98)00313-6.

Komaba, H., Fukagawa, M., 2016. Phosphate—a poison for humans? Kidney Int. 90, 753–763. https://doi.org/10.1016/j.kint.2016.03.039.

Kundu, S., Kawamura, K., Andreae, T.W., Hoffer, A., Andreae, M.O., 2010. Diurnal variation in the water-soluble inorganic ions, organic carbon and isotopic compositions of total carbon and nitrogen in biomass burning aerosols from the LBA-SMOCC campaign in Rondônia, Brazil. J. Aerosol Sci. 41. https://doi.org/10.1016/j.jaerosci.2009.08.006.

Lestari, P., Tasrifani, A.R., Suri, W.I., Wooster, M.J., Grosvenor, M.J., Fujii, Y., Ardiyani, V., Carboni, E., Thomas, G., 2024. Gaseous, particulate matter, carbonaceous compound, water-soluble ion, and trace metal emissions measured from 2019 peatland fires in Palangka Raya, Central Kalimantan. Atmos. Environ. 316. https://doi.org/10.1016/j.atmosenv.2023.120171.

Mahapatra, P.S., Panda, U., Mallik, C., Boopathy, R., Jain, S., Sharma, S.K., Mandal, T.K., Senapati, S., Satpathy, P., Panda, S., Das, T., 2021. Chemical, microstructural, and biological characterization of wintertime PM2.5 during a land campaign study in a coastal city of eastern India. Atmos. Pollut. Res. 12. https://doi.org/10.1016/j.apr.2021.101164.

Mahapatra, P.S., Sinha, P.R., Boopathy, R., Das, T., Mohanty, S., Sahu, S.C., Gurjar, B.R., 2018. Seasonal progression of atmospheric particulate matter over an urban coastal region in peninsular India: role of local meteorology and long-range transport. Atmos. Res. 199. https://doi.org/10.1016/j.atmosres.2017.09.001.

Maykut, N.N., Lewtas, J., Kim, E., Larson, T.V., 2003. Source apportionment of PM2.5 at an urban IMPROVE site in Seattle, Washington. Environ. Sci. Technol. 37. https://doi.org/10.1021/es030370y.

Mertoglu, E., Amantha, H.D., Flores-Rangel, R.M., 2022. Chemical characterization of water-soluble ions in highly time-resolved atmospheric fine particles in Istanbul megacity. Environ. Sci. Pollut. Control Ser. 29. https://doi.org/10.1007/s11356-022-21300-z.

Moufarrej, L., Courcot, D., Ledoux, F., 2020. Assessment of the PM2.5 oxidative potential in a coastal industrial city in Northern France: relationships with chemical composition, local emissions and long range sources. Sci. Total Environ. 748. https://doi.org/10.1016/j.scitotenv.2020.141448.

Naimabadi, A., Ghadiri, A., Idani, E., Babaei, A.A., Alavi, N., Shirmardi, M., Khodadadi, A., Marzouni, M.B., Ankali, K.A., Rouhizadeh, A., Rouhizadeh, A., Goudarzi, G., 2016. Chemical composition of PM_{10} and its in vitro toxicological impacts on lung cells during the Middle Eastern Dust (MED) storms in Ahvaz, Iran. Environ. Pollut. 211, 316–324. https://doi.org/10.1016/j.envpol.2016.01.006.

Niu, Y., Li, X., Qi, B., Du, R., 2022. Variation in the concentrations of atmospheric PM2.5 and its main chemical components in an eastern China city (Hangzhou) since the release of the Air Pollution Prevention and Control Action Plan in 2013. Air Qual Atmos Health 15. https://doi.org/10.1007/s11869-021-01107-6.

Organización Mundial de la Salud (OMS), 2021. WHO Global Air Quality Guidelines. Particulate Matter (PM2.5 and PM10), Ozone, Nitrogen Dioxide, Sulfur Dioxide and Carbon Monoxide.

Panda, S., Bikkina, S., Sharma, S.K., Das, T., Ramasamy, B., 2023. Chemical characterisation of fine aerosols in a smart city on the east coast of India: seasonal variability and its impact on visibility impairment. J. Earth Syst. Sci. 132. https://doi.org/10.1007/s12040-022-02043-4.

Paraskevopoulou, D., Liakakou, E., Gerasopoulos, E., Mihalopoulos, N., 2015. Sources of atmospheric aerosol from long-term measurements (5years) of chemical composition in Athens, Greece. Sci. Total Environ. 527–528. https://doi.org/10.1016/j.scitotenv.2015.04.022.

Pio, C., Alves, C., Nunes, T., Cerqueira, M., Lucarelli, F., Nava, S., Calzolai, G., Gianelle, V., Colombi, C., Amato, F., Karanasiou, A., Querol, X., 2020. Source apportionment of PM2.5 and PM10 by Ionic and Mass Balance (IMB) in a traffic-influenced urban atmosphere. Portugal. Atmos Environ 223. https://doi.org/10.1016/j.atmosenv.2019.117217.

Pipal, A.S., Tiwari, S., Satsangi, P.G., 2016. Seasonal chemical characteristics of atmospheric aerosol particles and its light extinction coefficients over Pune, India. Aerosol Air Qual. Res. 16. https://doi.org/10.4209/aaqr.2015.08.0529.

Pui, D.Y.H., Chen, S.-C., Zuo, Z., 2014. $PM_{2.5}$ in China: measurements, sources, visibility and health effects, and mitigation. Particuology 13, 1–26. https://doi.org/10.1016/j.partic.2013.11.001.

Rattanapotanan, T., Thongyen, T., Bualert, S., Choomanee, P., Suwattiga, P., Rungrattanaubon, T., Utavong, T., Phupijit, J., Changplaiy, N., 2023. Secondary sources of PM2.5 based on the vertical distribution of organic carbon, elemental carbon, and water-soluble ions in Bangkok. Environmental Advances 11. https://doi.org/10.1016/j.envadv.2022.100337.

Remoundaki, E., Kassomenos, P., Mantas, E., Mihalopoulos, N., Tsezos, M., 2013. Composition and mass closure of $PM_{2.5}$ in urban environment (Athens, Greece). Aerosol Air Qual. Res. 13, 72–82. https://doi.org/10.4209/aaqr.2012.03.0054.

Salma, I., Chi, X., Maenhaut, W., 2004. Elemental and organic carbon in urban canyon and background environments in Budapest, Hungary. Atmos. Environ. 38. https://doi.org/10.1016/j.atmosenv.2003.09.047.

Samara, C., Voutsa, D., Kouras, A., Eleftheriadis, K., Maggos, T., Saraga, D., Petrakakis, M., 2014. Organic and elemental carbon associated to PM10 and PM2.5 at urban sites of northern Greece. Environ. Sci. Pollut. Control Ser. 21. https://doi.org/10.1007/s11356-013-2052-8.

Saraga, D., Maggos, T., Sadoun, E., Fthenou, E., Hassan, H., Tsiouri, V., Karavoltsos, S., Sakellari, A., Vasilakos, C., Kakosimos, K., 2017. Chemical characterization of indoor and outdoor particulate matter ($PM_{2.5}$, PM_{10}) in Doha, Qatar. Aerosol Air Qual. Res. 17, 1156–1168. https://doi.org/10.4209/aaqr.2016.05.0198.

Schwarz, J., Pokorná, P., Rychlík, Š., Škáchová, H., Vlček, O., Smolík, J., Ždímal, V., Hůnová, I., 2019. Assessment of air pollution origin based on year-long parallel measurement of PM 2.5 and PM 10 at two suburban sites in Prague, Czech Republic. Sci. Total Environ. 664. https://doi.org/10.1016/j.scitotenv.2019.01.426.

Shahsavani, A., Naddafi, K., Jaafarzadeh Haghighifard, N., Mesdaghinia, A., Yunesian, M., Nabizadeh, R., Arhami, M., Yarahmadi, M., Sowlat, M.H., Ghani, M., Motevalian, S.A., Soleimani, Z., 2012. Characterization of ionic composition of TSP and PM_{10} during the middle eastern dust (MED) storms in Ahvaz, Iran. Environ. Monit. Assess. 184, 6683–6692. https://doi.org/10.1007/s10661-011-2451-6.

Sharma, S.K., Mandal, T.K., Jain, S., Saraswati, Sharma, A., Saxena, M., 2016. Source apportionment of PM2.5 in Delhi, India using PMF model. Bull. Environ. Contam. Toxicol. 97. https://doi.org/10.1007/s00128-016-1836-1.

Shon, Z.H., Ghosh, S., Kim, K.H., Song, S.K., Jung, K., Kim, N.J., 2013. Analysis of water-soluble ions and their precursor gases over diurnal cycle. Atmos. Res. 132–133. https://doi.org/10.1016/j.atmosres.2013.06.003.

Siciliano, T., Siciliano, M., Malitesta, C., Proto, A., Cucciniello, R., Giove, A., Iacobellis, S., Genga, A., 2018. Carbonaceous PM10 and PM2.5 and secondary organic aerosol in a coastal rural site near Brindisi (Southern Italy). Environ. Sci. Pollut. Control Ser. 25. https://doi.org/10.1007/s11356-018-2237-2.

Sillanpää, M., Frey, A., Hillamo, R., Pennanen, A.S., Salonen, R.O., 2005. Organic, elemental and inorganic carbon in particulate matter of six urban environments in Europe. Atmos. Chem. Phys. 5. https://doi.org/10.5194/acp-5-2869-2005.

Su, J., Zhao, P., Ding, J., Du, X., Dou, Y., 2021. Insights into measurements of water-soluble ions in PM2.5 and their gaseous precursors in Beijing. J. Environ. Sci. (China) 102. https://doi.org/10.1016/j.jes.2020.08.031.

Tao, J., Gao, J., Zhang, L., Zhang, R., Che, H., Zhang, Z., Lin, Z., Jing, J., Cao, J., Hsu, S. C., 2014. PM2.5 pollution in a megacity of Southwest China: source apportionment and implication. Atmos. Chem. Phys. 14. https://doi.org/10.5194/acp-14-8679-2014.

Tepe, A.M., Doğan, G., 2021. Chemical characterization of PM2.5 and PM2.5–10 samples collected in urban site in Mediterranean coast of Turkey. Atmos. Pollut. Res. 12, 46–59. https://doi.org/10.1016/j.apr.2020.08.012.

Tian, Y.Z., Xiao, Z.M., Han, B., Shi, G.L., Wang, W., Hao, H.Z., Li, X., Feng, Y.C., Zhu, T., 2013. Seasonal study of primary and secondary sources of carbonaceous species in PM10 from five northern Chinese cities. Aerosol Air Qual. Res. 13. https://doi.org/10.4209/aaqr.2012.01.0010.

Tolis, E.I., Saraga, D.E., Ammari, G.Z., Gkanas, E.I., Gougoulas, T., Papaioannou, C.C., Sarioglou, A.K., Kougioumtzidis, E., Skemperi, A., Bartzis, J.G., 2014. Chemical characterization of particulate matter (PM) and source apportionment study during winter and summer period for the city of Kozani, Greece. Cent. Eur. J. Chem. 12. https://doi.org/10.2478/s11532-014-0531-5.

Tran, N., Fujii, Y., Khan, M.F., Hien, T.T., Minh, T.H., Okochi, H., Takenaka, N., 2024. Source apportionment of ambient $PM_{2.5}$ in Ho chi Minh city, Vietnam. Asian Journal of Atmospheric Environment 18. https://doi.org/10.1007/s44273-023-00024-7.

Tsai, J.-H., Chen, S.-J., Lin, S.-L., Xu, Z.-Y., Huang, K.-L., Lin, C.-C., 2021. Chemical characterization of water-soluble ions and metals in particulate matter generated by a portable two-stroke gasoline engine. Aerosol Air Qual. Res. 21, 1–14. https://doi.org/10.4209/aaqr.200632.

Verma, S.K., Deb, M.K., Suzuki, Y., Tsai, Y.I., 2010. Ion chemistry and source identification of coarse and fine aerosols in an urban area of eastern central India. Atmos. Res. 95. https://doi.org/10.1016/j.atmosres.2009.08.008.

Viana, M., Chi, X., Maenhaut, W., Querol, X., Alastuey, A., Mikuška, P., Večeřa, Z., 2006. Organic and elemental carbon concentrations in carbonaceous aerosols during summer and winter sampling campaigns in Barcelona, Spain. Atmos. Environ. 40. https://doi.org/10.1016/j.atmosenv.2005.12.001.

Viana, M., Maenhaut, W., Chi, X., Querol, X., Alastuey, A., 2007a. Comparative chemical mass closure of fine and coarse aerosols at two sites in south and west Europe: implications for EU air pollution policies. Atmos. Environ. 41, 315–326. https://doi.org/10.1016/j.atmosenv.2006.08.010.

Viana, M., Maenhaut, W., ten Brink, H.M., Chi, X., Weijers, E., Querol, X., Alastuey, A., Mikuška, P., Večeřa, Z., 2007b. Comparative analysis of organic and elemental carbon concentrations in carbonaceous aerosols in three European cities. Atmos. Environ. 41. https://doi.org/10.1016/j.atmosenv.2007.03.035.

Vodička, P., Schwarz, J., Ždímal, V., 2013. Analysis of one year's OC/EC data at a Prague suburban site with 2-htime resolution. Atmos. Environ. 77. https://doi.org/10.1016/j.atmosenv.2013.06.013.

von Schneidemesser, E., Zhou, J., Stone, E.A., Schauer, J.J., Qasrawi, R., Abdeen, Z., Shpund, J., Vanger, A., Sharf, G., Moise, T., Brenner, S., Nassar, K., Saleh, R., Al-Mahasneh, Q.M., Sarnat, J.A., 2010. Seasonal and spatial trends in the sources of fine particle organic carbon in Israel, Jordan, and Palestine. Atmos. Environ. 44. https://doi.org/10.1016/j.atmosenv.2010.06.039.

Waked, A., Afif, C., Brioude, J., Formenti, P., Chevaillier, S., El Haddad, I., Doussin, J.F., Borbon, A., Seigneur, C., 2013. Composition and source apportionment of organic aerosol in Beirut, Lebanon, during winter 2012. Aerosol. Sci. Technol. 47. https://doi.org/10.1080/02786826.2013.831975.

Wang, Y., Zhuang, G., Tang, A., Yuan, H., Sun, Y., Chen, S., Zheng, A., 2005. The ion chemistry and the source of PM2.5 aerosol in Beijing. Atmos. Environ. 39. https://doi.org/10.1016/j.atmosenv.2005.03.013.

Wang, Z., Yan, J., Zhang, P., Li, Z., Guo, C., Wu, K., Li, X., Zhu, X., Sun, Z., Wei, Y., 2022. Chemical characterization, source apportionment, and health risk assessment of PM2.5 in a typical industrial region in North China. Environ. Sci. Pollut. Control Ser. 29. https://doi.org/10.1007/s11356-022-19843-2.

Williams, J., Petrik, L., Wichmann, J., 2021. PM2.5 chemical composition and geographical origin of air masses in Cape Town, South Africa. Air Qual Atmos Health 14. https://doi.org/10.1007/s11869-020-00947-y.

World Health Organisation, 2018. WHO global ambient air quality database (update 2018). Ambient Air Quality Database (Update 2018).

Yahaya, S.M., Mahmud, A.A., Abdullahi, M., Haruna, A., 2023. Recent advances in the chemistry of nitrogen, phosphorus and potassium as fertilizers in soil: a review. Pedosphere 33, 385–406. https://doi.org/10.1016/j.pedsph.2022.07.012.

Yamagami, M., Ikemori, F., Nakashima, H., Hisatsune, K., Ueda, K., Wakamatsu, S., Osada, K., 2021. Trends in PM2.5 concentration in Nagoya, Japan, from 2003 to 2018 and impacts of PM2.5 countermeasures. Atmosphere 12. https://doi.org/10.3390/atmos12050590.

Zhang, S., Wang, Z., Zhang, J., Guo, D., Chen, Y., 2021a. Inhalable cigarette-burning particles: size-resolved chemical composition and mixing state. Environ. Res. 202. https://doi.org/10.1016/j.envres.2021.111790.

Zhang, T., Cao, J.J., Tie, X.X., Shen, Z.X., Liu, S.X., Ding, H., Han, Y.M., Wang, G.H., Ho, K.F., Qiang, J., Qiang, J., Li, W.T., 2011. Water-soluble ions in atmospheric aerosols measured in Xi'an, China: seasonal variations and sources. Atmos. Res. 102, 110–119. https://doi.org/10.1016/j.atmosres.2011.06.014.

Zhang, W., Peng, X., Bi, X., Cheng, Y., Liang, D., Wu, J., Tian, Y., Zhang, Y., Feng, Y., 2021b. Source apportionment of PM2.5 using online and offline measurements of chemical components in Tianjin, China. Atmos. Environ. 244. https://doi.org/10.1016/j.atmosenv.2020.117942.

Zhou, J., Xing, Z., Deng, J., Du, K., 2016a. Characterizing and sourcing ambient PM2.5 over key emission regions in China I: water-soluble ions and carbonaceous fractions. Atmos. Environ. 135. https://doi.org/10.1016/j.atmosenv.2016.03.054.

Zhou, M., Qiao, L., Zhu, S., Li, L., Lou, S., Wang, H., Wang, Q., Tao, S., Huang, C., Chen, C., 2016b. Chemical characteristics of fine particles and their impact on visibility impairment in Shanghai based on a 1-year period observation. J. Environ. Sci. (China) 48. https://doi.org/10.1016/j.jes.2016.01.022.